Journal of Theoretical and Computational Chemistry, Vol. 1, No. 1 (2002) 109–136

RECENT ADVANCES IN ELECTRONIC STRUCTURE THEORY

TAKAHITO NAKAJIMA, TAKAO TSUNEDA,
HARUYUKI NAKANO and KIMIHIKO HIRAO*
Department of Applied Chemistry, School of Engineering, The University of Tokyo, Tokyo 113-8656, Japan
**hirao@qcl.t.u-tokyo.ac.jp*

Received 2 April 2002
Accepted 11 April 2002

Accurate quantum computational chemistry has evolved dramatically. The size of molecular systems, which can be studied accurately using molecular theory is increasing very rapidly. Theoretical chemistry has opened up a world of new possibilities. It can treat real systems with predictable accuracy. Computational chemistry is becoming an integral part of chemistry research. Theory can now make very significant contribution to chemistry.

This review will focus on our recent developments in the theoretical and computational methodology for the study of molecular structure and molecular interactions. We are aiming at developing accurate molecular theory on systems containing hundreds of atoms. We continue our research in the following three directions: (i) development of new *ab initio* theory, particularly multireference-based perturbation theory, (ii) development of exchange and correlation functionals in density functional theory, and (iii) development of molecular theory including relativistic effects.

We have enjoyed good progress in each of the above areas. We are very excited about our discoveries of new theory and new algorithms and would like to share this enthusiasm with readers.

Keywords: Correlation effects; DFT; relativistic effects; MRMP; MC-QDPT; RESC; DK3; OP and parameter-free functionals.

1. Multirference Based Perturbation Theory (MRPT)

Single reference many-body perturbation theory and coupled cluster (CC) theory are very effective in describing dynamical correlation, but fail badly in dealing with nondynamical correlation. Truncated CI can handle nondynamical correlation well, but configuration expansion in MRCI is quite lengthy and does not represent an optimal approach. Multireference technique can handle nondynamical correlation well. Once the state-specific nondynamical correlation is removed, the rest is primarily composed of dynamical pair correlation and individual pair correlation can be treated independently. So we implemented multireference based Rayleigh–Schrödinger perturbation approach with Møller–Plesset (MP) partitioning. MRPT is based on a concept of "different prescription for different correlation".

Multireference Møller–Plesset (MRMP)[1–4] and MC-QDPT (quasi-degenerate perturbation theory with multiconfiguration self-consistent field reference functions)[5,6] have opened up a whole new area and has had a profound impact on the potential of theoretical chemistry. MRMP and MC-QDPT have been successfully applied to numerous chemical and spectroscopic problems and have established as an efficient method for treating nondynamical and dynamical correlation effects. MRMP and MC-QDPT can handle any state, regardless of charge, spin, or symmetry, with surprisingly high and consistent accuracy.

*Corresponding author.

However, MRMP and MC-QDPT have sharp limit to the number of configurations of reference complete active space (CAS) SCF wave function.[7–9] To avoid this problem, we have developed perturbation theory (PT) based on the quasi-complete active space (QCAS) SCF wave function.[10,11] QCAS is defined as the product space of CAS spanned by the determinants or CSF. Numerical illustration shows that QCAS works quite well. However, QCAS requires physically sound judgment and/or intuition in the choice of subspace. Very recently we have presented a second-order PT starting with *general* multiconfiguration (MC) SCF wave functions.[12] The general MCSCF functions are wave functions optimized in an active space spanned by an arbitrary set of Slater determinants or configuration state functions (CSFs). The approach can dramatically reduce the dimension of the reference function.

MRMP with a complete active space configuration interaction (CASCI) reference function has also been proposed as an accurate and computationally efficient method for treating the ground and excited states of molecules.[13] The CASCI wave function is constructed using the SCF orbitals and used as a reference function of the MRMP to incorporate the remaining dynamical correlation. The advantage in using the CASCI is that it does not require iterations, nor does it encounter convergence difficulties that may be found in CASSCF calculations.

These recent advances will be reviewed in this section. First we will give a brief review of MRMP and MC-QDPT. Then PT with general MCSCF reference function and CASCI–MRMP will be discussed.

1.1. *The MRMP method— Multireference Møller–Plesset perturbation method*[1–4]

Our basic problem is to find approximations to some low-lying solutions of the exact Schrödinger equation,

$$H\Psi = E\Psi\,. \tag{1}$$

H is the Hamiltonian and it is decomposed into two parts, a zeroth-order Hamiltonian H_0 and a perturbation V,

$$H = H_0 + V\,. \tag{2}$$

We assume that a complete set of orthonormal eigenfunctions $\{\Psi_i^{(0)}\}$ and corresponding eigenvalues are available,

$$H_0\Psi_i^{(0)} = E_i^{(0)}\Psi_i^{(0)}\,. \tag{3}$$

Then the state wavefunction Ψ_I is expanded in terms of basis functions $\Psi_k^{(0)}$ as

$$\Psi_I = \sum_k C_{Ik}\Psi_k^{(0)}\,. \tag{4}$$

Some of the basis functions define an active space P and the remaining part of Hilbert space is called the orthogonal space $Q = 1 - P$. The active space is spanned by the basis functions that have a filled core and the remaining active electrons distributed over a set of active orbitals. The orthogonal complete space incorporates all other possible basis functions that are characterized by having at least one vacancy in a core orbital. The state wave function in an active space is written as

$$\Psi_I^{(0)} = \sum_k C_k\Phi_k \tag{5}$$

where the sum runs over active space basis functions $\{\Phi_i\}$ and C_k are the coefficients of only active space basis functions. It is convenient to use intermediate normalization, i.e.

$$\langle\Psi_I^{(0)}|\Psi_I^{(0)}\rangle = \langle\Psi_I^{(0)}|\Psi_I\rangle = 1\,. \tag{6}$$

We also assume that $\Psi_I^{(0)}$ is diagonal in P space,

$$\langle\Psi_I^{(0)}|H|\Psi_J^{(0)}\rangle = \delta_{IJ}(E_I^{(0)} + E_I^{(1)}) \tag{7}$$

with

$$E_I^{(0)} = \langle\Psi_I^{(0)}|H_0|\Psi_I^{(0)}\rangle \tag{8}$$

$$E_I^{(1)} = \langle\Psi_I^{(0)}|V|\Psi_I^{(0)}\rangle\,. \tag{9}$$

The state-specific Rayleigh–Schrödinger PT based on the unperturbed eigenvalue equation

$$H_0\Psi_I^{(0)} = E_I^{(0)}\Psi_I^{(0)} \tag{10}$$

leads to the first $E_I^{(k)}$ as

$$E_I^{(2)} = \langle\Psi_I^{(0)}|VRV|\Psi_I^{(0)}\rangle \tag{11}$$

$$E_I^{(3)} = \langle\Psi_I^{(0)}|VR(V - E_I^{(1)})RV|\Psi_I^{(0)}\rangle \tag{12}$$

$$\begin{aligned} E_I^{(4)} = {} & \langle\Psi_I^{(0)}|VR(V - E_I^{(1)})R(V - E_I^{(1)})RV|\Psi_I^{(0)}\rangle \\ & - E_I^{(2)}\lfloor\langle\Psi_I^{(0)}|VR^2V|\Psi_I^{(0)}\rangle \\ & + \langle\Psi_I^{(0)}|VRH_0SH_0RV|\Psi_I^{(0)}\rangle\rfloor \qquad \text{etc.} \end{aligned} \tag{13}$$

The R and S are the resolvent operators

$$R = Q/(E_I^{(0)} - H_0) \tag{14}$$

$$S = P'/(E_I^{(0)} - H_0) \tag{15}$$

where $P' = P - |\Psi_I^{(0)}\rangle\langle\Psi_I^{(0)}|$.

The $E_I^{(0)}$ is given in terms of orbital energies as

$$E_I^{(0)} = \sum_k D_{kk}\varepsilon_k \tag{16}$$

and the orbital energies are defined as

$$\varepsilon_i = \langle\varphi_i|F|\varphi_i\rangle \tag{17}$$

with

$$F_{ij} = h_{ij} + \sum_{kl} D_{kl}\left[(ij|kl) - \frac{1}{2}(il|kj)\right] \tag{18}$$

where D_{ij} is the one-electron density matrix. The MCSCF orbitals are resolved to make F_{ij} matrix as diagonal as possible. This zeroth-order Hamiltonian is closely analogous to the closed-shell Fock operator. The definition of an active space, the choices of active orbitals and the specification of the zeroth-order Hamiltonian completely determine the perturbation approximation.

When CASSCF wave function is used as the reference, the zeroth plus first order energy $E_I^{(0)} + E_I^{(1)}$ is equal to the CASSCF energy. The lowest non-trivial order is therefore the second order. Let the reference function $|\Psi_\alpha^{(0)}\rangle$ be a CASSCF wave function,

$$|\alpha\rangle = \sum_A C_A|A\rangle\,. \tag{19}$$

The energy up to the second order in MRMP is given by

$$E_\alpha^{(0-2)} = E_\alpha^{\mathrm{CAS}} + \sum_I \frac{\langle\alpha|V|I\rangle\langle I|V|\alpha\rangle}{E_\alpha^{(0)} - E_I^{(0)}} \tag{20}$$

where $\{|I\rangle\}$ is the set of all singly and doubly excited configurations from the reference configurations in CAS. The first term of the RHS is the CASCI energy.

1.2. *MC-QDPT— Multistate multireference perturbation method*[5,6]

We have also proposed a multistate multireference perturbation theory, the quasidegenerate perturbation theory with MCSCF reference functions (MC-QDPT). In this PT, state-averaged CASSCF is first performed to set reference functions, and then an effective Hamiltonian is constructed, which is finally diagonalized to obtain the energies of interest. This theory includes MRMP PT (the case that the set of reference functions reduces to a single function).

The effective Hamiltonian to second order is given by

$$(H_{\mathrm{eff}}^{(0-2)})_{\alpha\beta} = \langle\alpha|H|\beta\rangle + \frac{1}{2}\sum_I \left\{ \frac{\langle\alpha|V|I\rangle\langle I|V|\beta\rangle}{E_\beta^{(0)} - E_I^{(0)}} + \frac{\langle\beta|V|I\rangle\langle I|V|\alpha\rangle}{E_\alpha^{(0)} - E_I^{(0)}} \right\}. \tag{21}$$

Substituting the second-quantized operator into V, we obtain an explicit formula using molecular integrals and orbital energies instead of matrix elements,

$$\begin{aligned}(H_{\mathrm{eff}}^{(0-2)})_{\alpha\beta} = {} & E_\alpha^{\mathrm{CAS}}\delta_{\alpha\beta} - \sum_{pq,B}\langle\alpha|E_{pq}|B\rangle C_B(\beta) \\ & \times \sum_e \frac{u_{pe}u_{eq}}{\varepsilon_e - \varepsilon_q + \Delta E_{B\alpha}} \\ & - \sum_{pqrs,B}\langle\alpha|E_{pq,rs}|B\rangle C_B(\beta) \\ & \times \left[\sum_e \frac{u_{pe}g_{eqrs}}{\varepsilon_e - \varepsilon_q + \varepsilon_r - \varepsilon_s + \Delta E_{B\alpha}} \right. \\ & + \sum_e \frac{g_{pers}u_{eq}}{\varepsilon_e - \varepsilon_q + \Delta E_{b\alpha}} + \frac{1}{2} \\ & \left. \times \sum_{(a,b)} \frac{g_{parb}g_{aqbs}}{\varepsilon_a - \varepsilon_q + \varepsilon_b - \varepsilon_s + \Delta E_{B\alpha}} \right] \\ & - \sum_{qprstu,B}\langle\alpha|E_{qp,rs,tu}|B\rangle C_B(\beta) \\ & \times \sum_e \frac{g_{pers}g_{eqtu}}{\varepsilon_e - \varepsilon_q + \varepsilon_t - \varepsilon_u + \Delta E_{B\alpha}} \\ & + (\alpha \leftrightarrow \beta)\end{aligned} \tag{22}$$

with

$$g_{pqrs} = (pq|rs) \tag{23}$$

$$u_{pq} = (p|h - \delta_{pq}\varepsilon_p|q) - \sum_i^{\mathrm{doc}}(2g_{pqii} - g_{piiq}) \tag{24}$$

and

$$\Delta E_{B\alpha} = E_B^{(0)} - E_\alpha^{(0)} \tag{25}$$

the difference between the energies of the zeroth-order state and configuration. The orbital labels $\{i, j\}$, $\{a\}$, and $\{e\}$ are for doubly occupied, active, and external orbitals, respectively, and $\{a', b'\}$ run over both active and external orbitals, and the suffix of the generator $\{p, q, r, s, t, u\}$ run over only active orbitals. The terms including doubly occupied orbitals are omitted in this equation. See Ref. 5 for the full formula.

The formula including doubly occupied orbitals might look tedious. However, the energy can be calculated as just a sum of simple terms, hence rather simple. Neither diagonalization nor solution of linear equation for large-scale matrices is necessary.

The computation is done with the coupling coefficient driven method. These coupling coefficients are sparse and can be prescreened according to the condition,

$$(\nu_B^{pq\cdots rs})_{\alpha\beta} = \langle\alpha|E_{pq,\ldots,rs}|B\rangle C_B(\beta) > \delta \tag{26}$$

where $\delta = 1 \times 10^{-8}$ is usually sufficient to keep the energy accuracy better than 10^{-5} hartree.

Thus the multiple summation for active orbitals in Eqs. (10)–(12), and other terms, which seemingly scales as the power of the number of active orbitals, is actually diminished considerably. Note that the MRMP energy can also be calculated with the formula Eq. (22) by setting the number of the states to one.

1.3. *The perturbation theory based on the general MCSCF wave function*[12]

Although CASSCF-based PT is efficient, the dimension of the CAS active space grows very rapidly with the number of active electrons and orbitals. Even today, the maximum number of active orbitals that can be handled routinely in commonly used program packages is 14–16. This considerably restricts the possibility of MRPT.

To reduce the CAS dimension, we have proposed the quasi-complete active space (QCAS) SCF method.[10,11] QCAS is the product space of several CASs. The dimension of QCAS constructed from a set of active electrons and orbitals may be much smaller than that of CAS constructed from the same set of the electrons and orbitals. Using QCAS as reference in the perturbation theory, we may therefore extend active electrons and orbitals beyond the limit of CAS. However, it is not always possible to select an appropriate QCAS, depending on the molecular systems of interest.

We have presented a second-order QDPT using *general* multiconfiguration (MC) SCF wave functions as reference (hereafter, GMC-QDPT).[12] The general MCSCF functions are wave functions optimized in an active space spanned by an arbitrary set of Slater determinants or configuration state functions (CSFs). We use *general* MCSCF to distinguish it from that of specific forms like CAS-, QCAS-, and restricted active space (RAS) SCF.[14] No restriction on the form of variational space is imposed.

For MRPT at the second-order level, the computational algorithms are roughly classified into two. One is the sum-over-states method based on the CI Hamiltonian matrix elements, where the intermediate (or first-order interacting) configuration functions Φ_I are constructed by single and double excitations from the reference configurations, and then the matrix elements between the reference state(s) $\Psi_{\rm ref}$ and Φ_I, $\langle\Psi_{\rm ref}|H|\Phi_I\rangle$, are computed. Finally the energy is computed as the sum over the intermediate states according to the second-order formula. The other is a diagrammatic method, where the product of the perturbation operators is computed diagrammatically without using the first-order wave functions.

An important feature of the diagrammatic method is its compactness. The second-order energy (or effective Hamiltonian) is computed simply as sums of the product of molecular integrals, coupling-coefficient, CI coefficients, and inverse of zeroth-order-energy difference. It can be performed with relatively large basis sets and reference spaces. The construction of a first-order interacting space, which grows very rapidly with the number of active electrons and orbitals, is not necessary. However, the diagrammatic method can be applied only to a complete or quasi-complete reference function. On the other hand, the sum-over-states method has flexibility and can be applied to any reference function. The selection of the reference configuration is quite feasible in contrast to the diagrammatic method.

The computational method for GMC-QDPT adopted here is a composite method that combines

both sum-over-states and diagrammatic computational methods: the sum-over-states method is used for the excitations among active orbitals (internal excitations), while the diagrammatic method is used for the excitations including virtual or/and core orbitals (external excitations). Thus, the GMC-QDPT has both features, i.e., the compactness and flexibility.

There have been several PTs using general multiconfigurational functions: the configuration interaction by perturbation with multiconfigurational zeroth-order wave functions selected by iterative process (CIPSI) approach by Huron *et al.*,[15] MROPTn with a reduced model space method by Staroverov and Davidson,[16] MRPT for (RAS and) selected active space reference functions by Celani and Werner,[17] general MRPT (based on the generalized Møller–Plesset PT of Murphy and Messmer[18]) by Grimme and Waletzke,[19] and CIPSI by Cimiraglia.[20] These methods differ formally from the present GMC-QDPT. Computationally, most of these PTs employ the sum-over-states method, while only Cimiraglia.s method is diagram-based.

The *general configuration space* (GCS) is defined by a space that is spanned by an arbitrary set of Slater determinants or CSFs. The orbitals are partitioned into three categories as in the ordinary MCSCF method: the core orbitals are doubly occupied and the virtual orbitals are unoccupied in all the determinants/CSFs in GCS, while the active orbitals may be occupied or unoccupied. The reference wave functions used in the perturbation calculations are determined by MCSCF (or MC-CI) using GCS as a variational space:

$$|\alpha\rangle = \sum_{A\in \mathrm{GCS}} C_A(\alpha)|A\rangle\,. \tag{27}$$

The effective Hamiltonian up to the second order $H_{\mathrm{eff}}^{(0-2)}$ of Van Vleck perturbation theory with unitary normalization is given by

$$(H_{\mathrm{eff}}^{(0-2)})_{AB} = H_{AB} + \frac{1}{2}[\langle\Phi_A^{(0)}|HR_BH|\Phi_B^{(0)}\rangle + \langle\Phi_A^{(0)}|HR_AH|\Phi_B^{(0)}\rangle] \tag{28}$$

with

$$R_A = \sum_{I\notin \mathrm{ref}} |\Phi_I^{(0)}\rangle(E_A^{(0)} - E_I^{(0)})^{-1}\langle\Phi_I^{(0)}| \tag{29}$$

where $\Phi_A^{(0)}(\Phi_B^{(0)})$ and $\Phi_I^{(0)}$ are reference wave functions and a function in the complement space (Q) of the reference space (P), respectively, and $E_B^{(0)}$ and $E_I^{(0)}$ are zeroth-order energies of functions $\Phi_B^{(0)}$ and $\Phi_I^{(0)}$.

Adopting (state-averaged) MCSCF (or MC-CI) wave functions $\alpha(\beta)$ as reference functions $\Phi_A^{(0)}(\Phi_B^{(0)})$, which define the P space, Eq. (28) becomes

$$(H_{\mathrm{eff}}^{(0-2)})_{\alpha\beta} = E_\alpha^{\mathrm{MC-SCF}}\delta_{\alpha\beta} + \frac{1}{2}\sum_{I\notin \mathrm{GCS}} \times \left\{\frac{\langle\alpha|H|I\rangle\langle I|H|\beta\rangle}{E_\beta^{(0)} - E_I^{(0)}} + (\alpha\leftrightarrow\beta)\right\} \tag{30}$$

where I is now a determinant/CSF outside the GCS. The notation $(\alpha\leftrightarrow\beta)$ means interchange α with β from the first term in curly brackets. The complementary eigenfunctions of the MC-CI Hamiltonian and the determinants/CSFs generated by exciting electrons out of the determinants/CSFs in GCS are orthogonal to the reference functions and define the Q space. The functions in the space complementary to the P space in GCS, however, do not appear in Eq. (30) since the interaction between the complementary functions and the reference functions is zero. The GMC-QDPT computation scheme is similar to that of QCAS-QDPT.[11] We define here the corresponding CAS (CCAS) as a CAS constructed from the same active electrons and orbitals, that is, the minimal CAS that includes the reference GCS. The summation over I in Eq. (30) may be divided into the summations over determinants/CSFs outside CCAS and over the determinants/CSFs outside the GCS but inside CCAS:

$$\sum_{I\notin \mathrm{GCS}} = \sum_{I\notin \mathrm{CCAS}} + \sum_{I\in \mathrm{CCAS}\wedge\notin \mathrm{GCS}} \tag{31}$$

then the former second order term in Eq. (30) may be written as

$$(H_{\mathrm{eff}}^{(2)})_{\alpha\beta} = \sum_{I\notin \mathrm{CCAS}} \frac{\langle\alpha|H|I\rangle\langle I|H|\beta\rangle}{E_\beta^{(0)} - E_I^{(0)}} + \sum_{I\in \mathrm{CCAS}\wedge I\notin \mathrm{GCS}} \frac{\langle\alpha|H|I\rangle\langle|H|\beta\rangle}{E_\beta^{(0)} - E_I^{(0)}}\,. \tag{32}$$

The first term in Eq. (32) represents external excitations, while the latter term represents internal excitations.[11]

The external term may be further written as

$$(H_{\mathrm{ext}}^{(2)})_{\alpha\beta} = \sum_{A,B\in \mathrm{GCS}} C_A(\alpha)C_B(\beta)(H_{\mathrm{ext}}^{(2)})_{AB} \tag{33}$$

with

$$(H^{(2)}_{\rm ext})_{AB} = \sum_{I \notin {\rm CCAS}} \frac{\langle A|H|I\rangle\langle|H|B\rangle}{E^{(0)}_B - E^{(0)}_I + (E^{(0)}_\beta - E^{(0)}_B)} \tag{34}$$

where $(H^{(2)}_{\rm ext})_{AB}$ is the effective Hamiltonian in the determinant/CSFs basis in the conventional QDPT except for the energy shift, E, in the denominator. Since the second-order diagrams do not depend on the denominator, the second-order effective Hamiltonian Eq. (34) [hence, also Eq. (33)] is expressed by the same diagrams as the conventional QDPT.

For internal terms, the diagrammatic approach may not be applied. Instead, matrix operations for the Hamiltonian matrix are used:

$$(H^{(2)}_{\rm int})_{\alpha\beta} = \mathbf{v}^T(\alpha) \cdot \mathbf{w}(\beta) \tag{35}$$

with

$$\mathbf{v}_I(\alpha) = \sum_{A \in {\rm GCS}} \langle I|H|A\rangle C_A(\alpha) \tag{36}$$

$$\mathbf{w}_I(\beta) = \sum_{B \in {\rm GCS}} \langle I|H|B\rangle C_B(\beta)/(E^{(0)}_\beta - E^{(0)}_B)\,. \tag{37}$$

The intermediate determinants/CSFs I are constructed by exciting one or two electron(s) from the reference determinants/CSFs within the active orbital space. In general, the number of I is not large, and thus they may be managed in computer memory.

In the present implementation, we used Slater determinants rather than CSFs, differing from the original MC-QDPT.[5] Let $\{I_\alpha\}$ and $\{I_\beta\}$ be sets of alpha and beta strings appearing in the reference configurations, respectively. The reference space is defined by the beta string sets for each alpha string, $\{I_\beta[I_\alpha]\}$, and equivalently the alpha string sets for each beta string, $I_\alpha[I_\beta]$.

In the diagrammatic computation of the external terms, one-, two-, and three-body coupling coefficients (CCs) are necessary. The one-body CCs are classified into two types,

$$\langle I_\alpha|E^\alpha_{pq}|J_\alpha\rangle\langle I_\beta|J_\beta\rangle \quad \text{and} \quad \langle I_\alpha|J_\alpha\rangle\langle I_\beta|E^\beta_{pq}|J_\beta\rangle$$

the two-body CCs into three types,

$$\langle I_\alpha|E^\alpha_{pq,rs}|J_\alpha\rangle\langle I_\beta|J_\beta\rangle, \langle I_\alpha|J_\alpha\rangle\langle I_\beta|E^\beta_{pq,rs}|J_\beta\rangle, \quad \text{and}$$
$$\langle I_\alpha|E^\alpha_{pq}|J_\alpha\rangle\langle I_\beta|E^\beta_{rs}|J_\beta\rangle$$

and the three-body CCs into four types,

$$\langle I_\alpha|E^\alpha_{pq,rs,tu}|J_\alpha\rangle\langle I_\beta|J_\beta\rangle, \langle I_\alpha|J_\alpha\rangle\langle I_\beta|E^\beta_{pq,rs,tu}|J_\beta\rangle$$
$$\langle I_\alpha|E^\alpha_{pq,rs}|J_\alpha\rangle\langle I_B|E^\beta_{tu}|J_\beta\rangle, \quad \text{and}$$
$$\langle I_\alpha|E^\alpha_{pq}|J_\alpha\rangle\langle I_\beta|E^\beta_{rs,tu}|J_\beta\rangle$$

with $J_\alpha \in \{I_\alpha\}$, $J_\beta \in \{I_\beta\}$ and

$$E^\alpha_{pq,rs,\ldots} = a^+_{p\alpha}a^+_{r\alpha}\cdots a_{s\alpha}a_{q\alpha} \tag{38}$$

$$E^\beta_{pq,rs,\ldots} = a^+_{p\beta}a^+_{r\beta}\cdots a_{s\beta}a_{q\beta}\,. \tag{39}$$

Since string $J_\alpha(J_\beta)$ is determined by string $I_\alpha(I_\beta)$ and active orbital labels p and q, the one-body CCs for strings, $\langle I_\alpha|E^\alpha_{pq}|J_\alpha\rangle(\langle I_\beta|E^\beta_{pq}|J_\beta\rangle)$, can be stored in the computer memory in the form $J_\alpha[I_\alpha;p,q]J_\beta[I_\beta;p,q]$. The perturbation calculation for three-body CCs, $\langle I_\alpha|E^\alpha_{pq,rs}|J_\alpha\rangle\langle I_\beta|E^\beta_{tu}|J_\beta\rangle$, for example, is done as follows:

```
Loop over I_α
Make all non-zero ⟨I_α|E^α_{pq,rs}|J_α⟩ for I_α
    Loop over I_β[I_α]
        Loop over t and u
            If J_β[I_α;t,u] ≠ 0 and J_β[I_α;t,u]
            ∈ {I_β[J_α]}, then
                do 3-body PT calculations for
                ⟨I_α|E^α_{pq,rs}|J_α⟩⟨I_β|E^β_{tu}|J_β⟩
        end loop t and u
    end loop I_β[I_α]
end loop I_α
```

The other terms can be computed similarly.

The one- and two-body CCs computed in the same manner are used for the CI based calculation for the internal terms. The vectors $\mathbf{v}_I$ in Eq. (35) are computed as σ-vectors using strings.

We applied GMC-QDPT to the calculation of the PECs of the two lowest $^1\Sigma^+$ states of the LiF molecule. In the diabatic picture, one of the $^1\Sigma^+$ states is ionic and the other is covalent. In the equilibrium structure region, the ionic state is lower in energy (the ground state), while at the dissociation limit the covalent state becomes lower. The two potential curves therefore show avoided-crossing in the middle of the adiabatic picture.

The basis set used was 6-311++G($3df, 3pd$).[21] The reference spaces were made by exciting one and

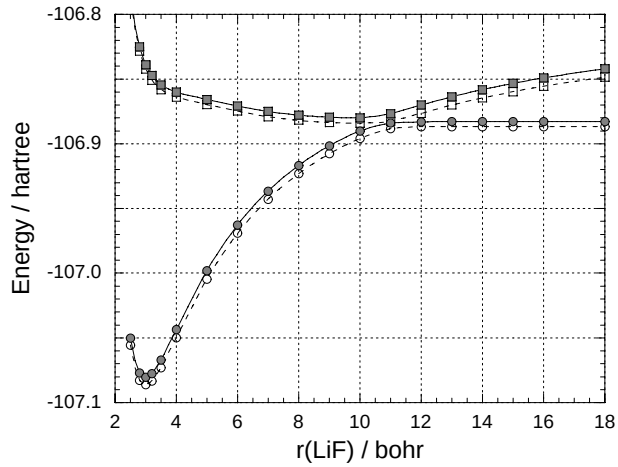

Fig. 1. The MCSCF (•, ■) and CASSCF (○, □) potential energy curves of the two lowest $^1\Sigma^+$ state of LiF.

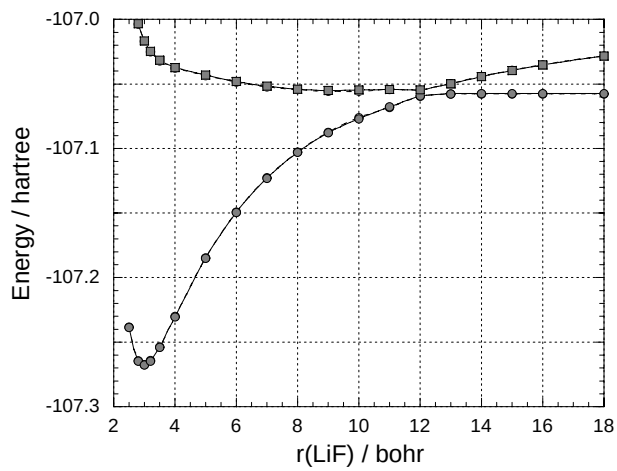

Fig. 2. The GMC-QDPT (•, ■) and CAS-QDPT (○, □) potential energy curves of the two lowest $^1\Sigma^+$ states of LiF.

two electrons from two parent configurations: the Hartree Fock and $4\sigma \rightarrow 5\sigma^*$ excitation configurations. The CAS and QCAS used for comparison were CAS(6, 9), and QCAS[$(2, 3)^3$], respectively, where in QCAS the division of the nine orbitals were $\{4\sigma - 6\sigma\}$, $\{1\pi - 3\pi\}$, and $\{1\pi' - 3\pi'\}$. The dimension of GCS was 241, and those of CAS and QCAS were 1812 and 729 (in Slater determinant basis; with symmetry), respectively. The 1σ orbital corresponding to F($1s$) was frozen in the perturbation calculations.

Results are shown in Figs. 1 and 2. Figure 1 shows PECs at the MCSCF and CASSCF levels and Fig. 2 shows PECs at the GMC-QDPT and CAS-QDPT levels. The MCSCF curves have systematic errors from the CAS-SCF results depending on the nature of the states: about 4 kcal mol^{-1} for the ionic state (in the diabatic picture; lower near the equilibrium structure, higher at the dissociation limit) and about 2.5 kcal mol^{-1} for the covalent state. These are recovered well by GMC-QDPT. At this level, the errors from CAS-QDPT are less than 1 kcal mol^{-1} for both states.

The next example is the calculation of valence excitation energies for formaldehyde molecule. Calculations on formaldehyde were carried out at the ground state experimental geometry[22] (i.e. r(CO) = 1.203 Å, r(CH) = 1.099 Å, and θ(HCH) = 116.5 degrees). The basis set used was Dunning's cc-pVTZ.[23]

Five reference spaces were constructed from 8 electrons, 16[$(a_1, a_2, b_1, b_2) = (7, 1, 3, 5)$], 18[$= (7, 1, 4, 6)$], 20[$= (8, 1, 5, 6)$], 22[$= (8, 2, 5, 7)$], and 24 orbitals [$= (9, 2, 6, 7)$], by exciting one and two electrons from the following parent configurations:

$^1A_1$ states : $\ldots n^2$(HF); $\quad \pi \rightarrow \pi^*$; $\quad n \rightarrow \sigma^*$

$^3A_1$ states : $\pi \rightarrow \pi^*$; $\quad n \rightarrow \sigma^*$

$^{1,3}A_2$ states : $n \rightarrow \pi^*$; $\quad 1b_2(\sigma) \rightarrow \pi^*$

$^{1,3}B_1$ states : $5a_1(\sigma) \rightarrow \pi^*$

$^{1,3}B_2$ states : $n \rightarrow 6a_1(\sigma^*)$.

The dimensions of the reference spaces, for example, in singlet A_1 were 3045, 4121, 5349, 6833, and 8413 for 16, 18, 20, 22, and 24 active orbitals, respectively: the dimensions increase like an arithmetic progression. The corresponding dimensions of symmetry-adapted CASs were 828,720 ($n_{\rm act} = 16$), 2,342,000 (= 18), 5,871,601 (= 20), 13,380,441 (= 22), and 28,234,186 (= 24). This increases much more rapidly than the GCS cases. All the calculations were done in each symmetry.

The results are summarized in Table 1. The results are compared in Table 2 to the available experiment and previous theoretical results, i.e., MRCI results by Hachey *et al.*,[24] the second-order complete active space perturbation theory (CASPT2) calculations by Merchán and Roos,[25] and the equation of motion coupled cluster (EOM-CC) calculations by Gwaltney *et al.*[26]

Table 1. Valence excitation energies of H_2CO (eV)

State	Orbital Picture	MC-SCF (8,16)	(8,18)	(8,20)	(8,22)	(8,24)	GMC-QDPT (8,16)	(8,18)	(8,20)	(8,22)	(8,24)	Exptl.
$^1A_1$	$\pi \to \pi^*; n \to \sigma^*$	10.07	10.03	10.03	10.02	10.02	9.66	9.67	9.72	9.72	9.72	
	$n \to \sigma^*; \pi \to \pi^*$	11.01	11.01	11.00	11.03	11.01	10.65	10.63	10.65	10.63	10.64	10.70
$^1A_2$	$n \to \pi^*$	4.32	4.43	4.27	4.25	4.22	4.04	4.02	4.01	4.02	4.08	4.07
	$1b_2(\sigma) \to \pi^*$	10.96	11.16	10.97	10.98	10.94	10.30	10.34	10.33	10.37	10.43	
$^1B_1$	$5a_1(\sigma) \to \pi^*$	9.63	9.89	9.82	9.81	9.80	9.31	9.24	9.26	9.20	9.28	9.00
$^1B_2$	$n \to 6a_1(\sigma^*)$	7.73	8.16	8.22	8.32	8.31	8.31	8.23	8.41	8.45	8.45	
$^3A_1$	$\pi \to \pi^*; n \to \sigma^*$	6.18	6.28	6.19	6.13	6.11	6.13	6.13	6.18	6.17	6.18	6.00
	$n \to \sigma^*; \pi \to \pi^*$	9.66	9.64	9.70	9.74	9.75	9.60	9.61	9.62	9.62	9.62	
$^3A_2$	$n \to \pi^*$	3.84	3.95	3.78	3.75	3.71	3.63	3.58	3.58	3.61	3.63	3.50
	$1b_2(\sigma) \to \pi^*$	10.52	10.68	10.52	10.52	10.47	10.04	10.03	10.02	10.07	10.10	
$^3B_1$	$5a_1(\sigma) \to \pi^*$	8.78	9.02	8.92	8.91	8.90	8.45	8.41	8.39	9.27	8.50	8.50
$^3B_2$	$n \to 6a_1(\sigma^*)$	7.36	7.79	7.85	7.95	7.94	7.89	7.80	7.99	8.02	8.07	

Table 2. Valence excitation energies of H_2CO (eV)

State	Orbital picture	MC-SCF (8,24)	GMC-QDPT (8.24)	Exptl.	MRCI[a]	CASPT2[b]	EOM-CC[c]	CCSD[d]	CIS-MP2[e]	SAC-CI[f]
$^1A_1$	$\imath \to \pi^*, n \to \sigma^*$	10.02	9.72		9.60	9.77	9.47	9.27	9.19	—
	$n \to \sigma^*, \pi \to \pi^*$	11.01	10.64	10.70						10.83
$^1A_2$	$n \to \pi^*$	4.22	4.08	4.07	4.05	3.91	3.98	3.95	4.58	4.16
	$1b_2(\sigma) \to \pi^*$	10.94	10.43				10.38		10.08	11.19
$^1B_1$	$5a_1(\sigma) \to \pi^*$	9.80	9.28	9.00	9.35	9.09	9.33	9.26	9.97	9.49
$^1B_2$	$n \to 6a_1(\sigma^*)$	8.31	8.45							
$^3A_1$	$\pi \to \pi^*; \pi \to \sigma^*$	6.11	6.18	6.00		5.99			6.72	6.10
	$n \to \sigma^*; \pi \to \pi^*$	9.75	9.62							
$^3A_2$	$n \to \pi^*$	3.71	3.63	3.50		3.48			4.15	3.70
	$1b_2(\sigma) \to \pi^*$	10.47	10.10						10.52	10.80
$^3B_1$	$5a_1(\sigma) \to \pi^*$	8.90	8.50	8.50					9.18	8.52
$^3B_2$	$n \to 6a_1(\sigma^*)$	7.94	8.07							

[a]M.R.J. Hachey, P.J. Bruna and F.J. Grein, *Phys. Chem.* **99**, 8050 (1995).
[b]M. Merchán and B.O. Roos, *Theor. Chim. Acta.* **92**, 227 (1995).
[c]S.R. Gwaltney and R.J. Bartlett, *Chem. Phys. Lett.* **241**, 26 (1995).
[d]C.M. Hadad, J.B. Foresman and K.B. Wiberg, *J. Phys. Chem.* **97**, 4293 (1993).
[e]M. Head-Gordon, R.J. Rico, M. Oumi and T.J. Lee, *Chem. Phys. Lett.* **219**, 21 (1994).
[f]H. Nakatsuji, K. Ohta and K. Hirao, *J. Chem. Phys.* **75**, 2952 (1981).

The maximum energy differences for the largest three (two) numbers of active orbitals is 0.09 (0.05) eV. We can therefore consider that the excitation energies at the MCSCF level are almost converged values for the change of the active orbital numbers. However, the agreement with the experimental values is not so good: the error is 0.32 eV on average and 0.80 eV at maximum.

At the GMC-QDPT level, the excitation energies are also almost converged. Compared to the reference MCSCF level, the results are somewhat improved. The error from the experimental value was reduced to 0.11 eV on average and 0.28 eV at maximum.

Theoretical results by multireference methods (MRCI and CASPT2) and EOM-CC are also available for several low-lying states. Harchey *et al.*[24]

presented the MRCI results for four singlet states [1^1A_2 (4.05 eV), 1^1B_1 (9.35 eV), and 2^1A_1 (9.60 eV) states], Merchén *et al.*[25] reported the CASPT2 results for three singlet and two triplet states [1^1A_2 (3.91 eV), 1^1B_1 (9.09 eV), 2^1A_1 (9.77 eV), 1^3A_2 (3.48 eV), and 2^3A_1 (5.99 eV) states], and Gwaltney *et al.*[26] gave the EOM-CC results for four singlet states [1^1A_2 (3.98 eV), 1^1B_1 (9.33 eV), 2^1A_1 (9.47 eV), and 2^1A_2 (10.38 eV) states]. These values are all close to the GMC-QDPT values, supporting the present results.

To conclude, the second-order QDPT with CAS reference functions was extended to the general MCSCF reference functions case, i.e. GMC-QDPT. There is no longer any restriction on the form of the reference space. It can treat more active orbitals and electrons than a CAS reference PT and thus is applicable to larger systems, and it can avoid unphysical multiple excited configurations, which are often responsible for the intruder state problem.

A computational scheme utilizes both diagrammatic and CI matrix-based sum-over-states approaches. The second-order GMC-QDPT effective Hamiltonian is computed for the external (outside CAS) and internal (inside CAS) intermediate configurations separately. For external intermediate configuration, the diagrammatic approach is used, which has been used for CAS- and QCAS-QDPT. The diagrams are identical to those of the original MC-QDPT and QCAS-QDPT; only the computational scheme of coupling constants is different. For the internal intermediate configurations, a CI matrix based method is used. The vectors used belong to MRSDCI space within active orbitals and therefore small enough to be easily treatable.

1.4. *The CASCI–MRMP method*[13,27]

Usually, CASSCF wave function is chosen as a reference function of MRMP. However, CASSCF often generates far too many configurations, and suffers from the convergence difficulties, particularly with an increasing size of the active space. CASSCF involves an iterative scheme, and a two-electron MO integral transformation and a matrix diagonalization are repeated in each iteration. This makes the MRMP method less efficient when dealing with large systems.

A single reference second-order MP method works fairly well when the Hartree–Fock wave function is a good approximation. It breaks down only when the nondynamical correlation is significant. As known well, the convergence of the dynamical correlation is rather slow, and the accurate representation of the dynamical correlation requires high levels of excitations in the many-electron wave function and high levels of polarization functions in a basis set. However, the situation is quite different for nondynamical correlation. The nondynamical, near-degeneracy effect converges fairly smoothly with respect to both the one-electron basis function and the many-electron wave function. This implies that the near-degeneracy problem can be handled quite well even in a moderate function space. This suggests the use of SCF orbitals instead of optimized CASSCF orbitals in MRMP calculations.

A CASCI wave function retains the attractive feature of the CASSCF wave function. The CASCI is a full CI (FCI) in a given active space. It is well defined, and has an upper bounds nature to the energies of the states. The CASCI can handle the near-degeneracy problem in a balanced way, and can be applied to the calculations of potential energy surfaces and excited states. It is size-consistent and the wave function is invariant to transformations among active orbitals. The principal advantages of using the CASCI are that it does not require iterations, and does not encounter convergence difficulties, as it is often found in excited state or state-averaged CASSCF calculations.

A reference CASCI wave function is obtained by partitioning the SCF occupied and virtual orbitals into doubly occupied core and active orbitals, and optimizing only the expansion coefficients of all configurations generated by all the possible arrangement of the active electrons among the active orbitals. In the case of CASSCF, the active orbitals in addition to the expansion coefficients of all configurations are also optimized through the SCF scheme.

The CASCI–MRMP scheme is applied to the potential curves of ground and low-lying excited states of N_2 and compared to the FCI results of Larsen *et al.*[28] We used the same cc-pVDZ basis set of Dunning *et al.*[29] as FCI calculations and the N 1*s* core orbital was frozen. The active orbitals of $(10, 10)$ consisted of $2\sigma_g - 3\sigma_g$, $2\sigma_u - 3\sigma_u$, $1\pi_g - 3\pi_g$ and $1\pi_u - 3\pi_u$ orbitals. All the excited states considered here are singly excited states around equilibrium, and the dominant single excitations are $3\sigma_g \rightarrow 1\pi_g$, $1\pi_u \rightarrow 1\pi_g$, and $1\pi_u \rightarrow 1\pi_g$ for $^1\Pi_g$, $^1\Sigma_u^-$, and $^1\Delta_u$ states,

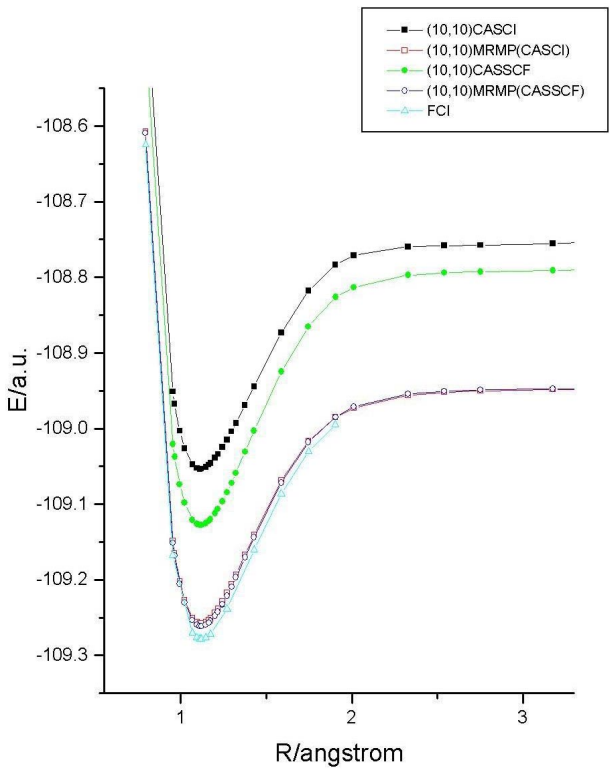

Fig. 3. Potential energy curve of the ground state of N_2 as computed by the CASCI (■), CASSCF (•), CASCI–MRMP (□), CASSCF-MRMP (○), and FCI (□) methods.

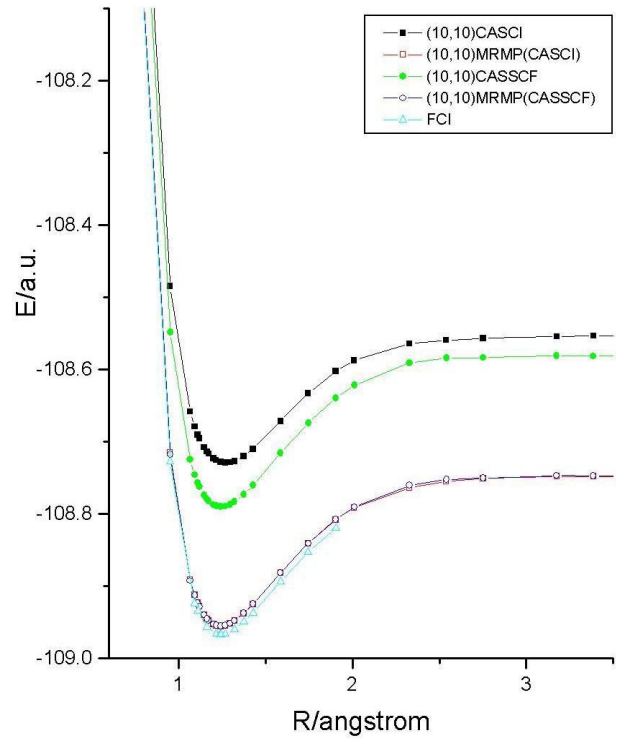

Fig. 4. Potential energy curve of the $^1\Pi_g$ state of N_2 as computed by the CASCI (■), CASSCF (•), CASCI–MRMP (□), CASSCF-MRMP (○), and FCI (□) methods.

respectively. The main features of the potential curves are common for all three excited states. In all three cases, one electron is excited from a bonding to an antibonding orbital. Thus, the bond lengths become larger than for the ground state.

Figure 3 shows the ground state potential curves calculated by CASCI, CASSCF, CASSCF-MRMP, CASCI–MRMP, and FCI methods. The CASCI and CASSCF curves contain no substantial qualitative defects, indicating that both methods can handle non-dynamical correlation quite well. Starting with these functions as a reference, we applied a perturbation treatment to include the remaining dynamical correlation, and obtained the CASCI–MRMP and CASSCF-MRMP curves. It is surprising that the difference between the two curves at the MRMP level is too small to be visible on the scale shown in Fig. 3, and both curves are quite close to the FCI curve. The CASCI method is apparently quite poor when compared with the CASSCF, but the deficiency is recovered well at the level of MRMP. The maximum energy difference between the CASCI and FCI methods is about 47 kcal mol^{-1} near to equilibrium, and is reduced to 2.4 kcal mol^{-1} at the MRMP level.

The CASCI–MRMP gives $R_e = 1.1187$ Å, $\omega_e = 2311$ cm^{-1}, and $D_e = 8.39$ eV for the ground state. The corresponding values of the CASSCF-MRMP calculations are $R_e = 1.1194$ Å, $\omega_e = 2309$ cm^{-1}, and $D_e = 8.61$ eV. The agreement with the FCI values ($R_e = 1.201$ Å, $\omega_e = 2323$ cm^{-1}, and $D_e = 8.74$ eV) is excellent. The MRMP with the CASCI is comparable in accuracy with the MRMP with the CASSCF.

The potential energy curves for the exited $^1\Pi_g$, $^1\Sigma_u^-$, and $^1\Delta_u$ states are shown in Figs. 4–6, respectively. These figures demonstrate that the same accuracy is obtained for the excited states. The CASCI–MRMP and CASSCF-MRMP methods give very close potential curves and are parallel to the corresponding FCI curves. Spectroscopic constants also show excellent agreement with those from the FCI method.

We also calculated the valence $\pi \rightarrow \pi^*$ excited states of benzene using the CASCI–MRMP method and compared the results with previous CASSCF-MRMP calculations.[30] Both singlet and triple

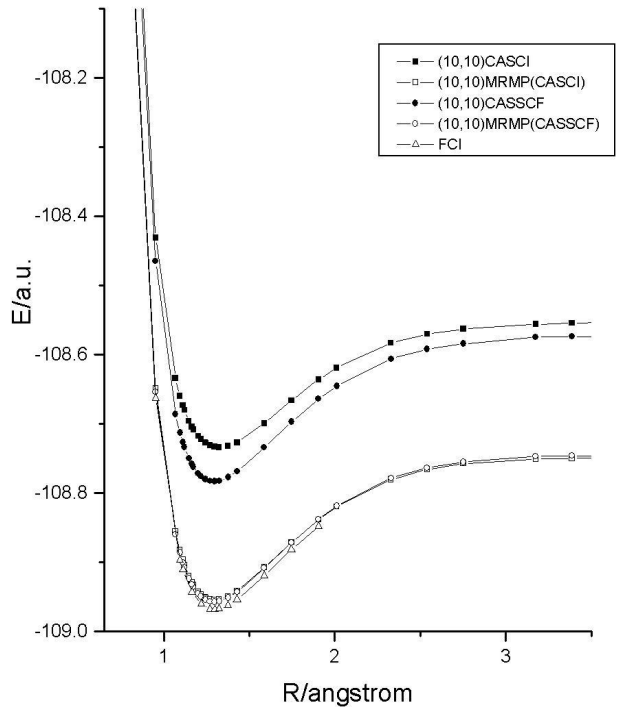

Fig. 5. Potential energy curve of the $^1\Sigma_u$ state of N_2 as computed by the CASCI (■), CASSCF (•), CASCI–MRMP (□), CASSCF-MRMP (○), and FCI (□) methods.

excitation energies were calculated. The molecule was placed in the xy plane. We used the same molecular structure as in the previous study with C–C and C–H bond lengths of 1.395 and 1.085 Å, respectively. We used the same basis set as the previous study: Dunning's cc-pVTZ basis set for carbon and cc-pVDZ[23] for hydrogen atoms were used, augmented with Rydberg functions $(8s8p8d/1s1p1d)$ placed at the center of the molecule. The 6π electrons were distributed among the 12π orbitals, $(6, 12)$ active space, in the CASCI calculation.

Table 3 summarizes the computed CASCI and CASCI–MRMP excitation energies. The CASSCF and CASSCF-MRMP results are also listed for comparison. The agreement between the CASCI–MRMP and CASSCF-MRMP results is excellent. The overall accuracy of the CASCI–MRMP method is surprisingly high. The excitation energies calculated by the CASCI–MRMP method are predicted with an accuracy of 0.09 eV for valence $\pi \rightarrow \pi^*$ singlet states, and 0.15 eV for valence triplet states. This accuracy is comparable to that of the MRMP method starting with averaged CASSCF wave functions.

The CASCI method tends to overestimate the excitation energies for the experimental values as the CASSCF method also does. The largest deviation, which is more than 1 eV, is found in the ionic *plus* states for both singlet and triplet states. The CASCI–MRMP method corrects the deficiency, and is a great improvement over the CASCI results. The MRMP excitation energies are quite close to the experimental values for both ionic *plus* and covalent *minus* states. For the ionic *plus* excited states, the dynamic σ–π polarization effect is much more significant than that of covalent *minus* states. Incorporation of the dynamical correlation by perturbation theory lowers the excitation energies by more than 1 eV. The CASCI–MRMP results slightly underestimate the excitation energies for the ionic *plus* states compared with those of the CASSCF-MRMP method. Although the fourth excited state, $1^1E_{2g}^-$, has a character of doubly excited nature, the CASCI–MRMP method has no difficulty in describing the doubly excited state.

The present calculations clearly demonstrate that the excited states are well represented by the MRMP method with a CASCI reference function constructed over SCF orbitals.

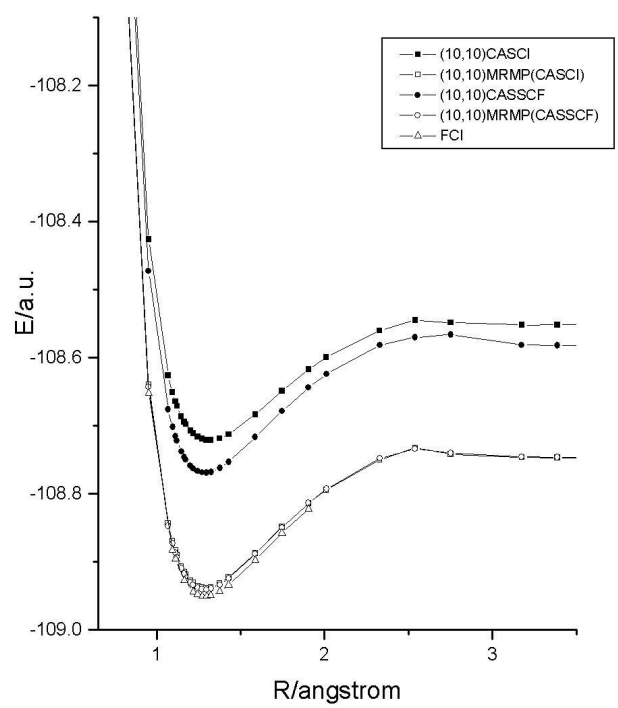

Fig. 6. Potential energy curve of the $^1\Delta_u$ state of N_2 as computed by CASCI (■), CASSCF (•), CASCI–MRMP (□), CASSCF-MRMP (○), and FCI (□) methods.

Table 3. Vertical $\pi - \pi^*$ excitation energies (eV) of benzene.

State	CASCI	CASSCF[a]	CASCI–MRMP	CASSCF-MRMP[a]	Exptl.[b]
$^1B_{2u}^-$	5.01	4.94	4.72	4.70	4.90
$^1B_{1u}^+$	7.58	7.55	6.14	6.21	6.20
$^1E_{1u}^+$	8.87	8.77	6.85	6.93	6.94
$^1E_{2g}^-$	8.17	8.05	7.81	7.82	7.80
$^3B_{1u}^-$	3.98	3.89	3.92	3.89	3.95
$^3E_{1u}^-$	4.92	4.85	4.52	4.53	4.76
$^3B_{2u}^+$	6.83	6.77	5.46	5.54	5.60
$^3E_{2g}^-$	7.27	7.16	7.06	7.02	6.83

[a]Ref. 30.
[b]Ref. 31 for $^1B_{2u}^-$, $^1B_{1u}^+$, and $^1E_{1u}^+$ states; Ref. 32 for $^1E_{2g}^-$ state; Ref. 33 or $^3B_{1u}^-$, $^3E_{1u}^-$, and $^3B_{2u}^+$ states; Ref. 34 for $^3E_{2g}^-$ state.

2. Density Functional Theory

In the field of computational chemistry, density functional theory (DFT) usually indicates the Kohn–Sham method that solves electron configurations of molecules by using the nonlinear Kohn–Sham equation with an exchange-correlation functional.[35–37] Compared to high-level *ab initio* molecular orbital theories, DFT is much simpler and requires much less computational timings to give equivalent chemical properties. DFT, therefore, becomes widely used to support experimental results from a theoretical point of view. However, it is not so far proved why DFT estimates highly accurate chemical properties. The most persuasive account may be that DFT incorporates well-balanced dynamical and nondynamical electron correlations. Compared Kohn–Sham potentials of the *ab initio* multireference configuration interaction method[38] with those of DFT, it was found that dynamical and nondynamical correlations are given by correlation and exchange functionals, respectively.[39] We should notice that chemical situations essentially stem from the changes of electron configurations due to transfers, increases and decreases of electrons. It is, therefore, necessary for accurate chemical calculations to keep the balance of parallel-spin (dynamical) and opposite-spin (nondynamical) electron-pair correlations in exchange-correlation functionals.

Most conventional exchange-correlation functionals are derived from a parametrized form that satisfies fundamental conditions of the exact functional with supplementary functions. The parameters are then determined by a semi-empirical fit to experimental chemical properties.[40–43] However, we should notice that this is the second best policy on the ground of the fixed idea that a semi-empirical fit is necessary to construct a sophisticated functional. A functional, essentially, should give either fundamental conditions or accurate chemical properties without a fit to these values. Recently, Tsuneda and Hirao developed parameter-free (Pfree) exchange[44] and one-parameter progressive (OP) correlation[45,46] functionals on the basis of the density matrix expansion and the Colle–Salvetti correlation wavefunction. Pfree and OP functionals contain updatable kinetic energy density and exchange functional terms, respectively. By applying the exact limit conditions to these terms, it is, surprisingly, proved that these functionals satisfy all significant conditions except for the long-range exchange asymptotic behavior.[44,45] It should be noted that these conditions are not taken into account in these functionals. This may indicate that fundamental conditions of kinetic, exchange, and correlation functionals are transversely connected through Pfree and OP functionals.[47] It was also confirmed that Pfree and OP functionals give equivalent-or-more accurate chemical properties compared to conventional functionals, despite that these functionals contain a minimum of parameters; no parameter for Pfree and one parameter for OP. Pfree and OP functionals and the transversing connection are briefly summarized in Sec. 2.1.

The self-interaction error (SIE) in exchange functionals may be one of the most serious problems

in DFT.[36,48] SIE originates from exchange self-interactions that are not cancelled out with Coulomb self-interactions due to one-electron potential approximations of conventional exchange functionals.[48–50] Pfree exchange functional also contains SIE resulted from the density matrix expansion. Although some conventional self-interaction correction (SIC) schemes have been suggested, most of these schemes intend to remove SIE on the basis of electron orbital from functionals of electron density. The discord of orbital and density may cause poor reproducibilities and time-consuming procedures. Recently, Tsuneda, Kamiya and Hirao proposed a regional self-interaction correction (RSIC) scheme that substitutes exchange self-interaction energies only for exchange functionals in self-interaction regions.[51] Since the RSIC scheme contains neither orbital-localizations nor transformations to an orbital-dependent form, we can obtain self-interaction corrected results based on the usual Kohn–Sham scheme. By applying RSIC to the calculations of chemical reaction barriers, it was found that underestimated barriers are obviously improved by this scheme. This RSIC scheme is outlined in Sec. 2.2.1.

Exchange-correlation functionals have problems that may not be interpreted by SIE. The most remarkable example may be the difficulties of Van der Waal's (VdW) calculations.[36] DFT studies show that it may be hard to obtain accurate Vdw bonds by using conventional functionals even if VdW correlation effects are taken into account in correlation functionals.[52] It was supposed that this maybe due to the lack of two-electron long-range interactions in exchange functionals. Despite the long-range interaction which maybe significant in the description of VdW bonds, it is essentially hard to incorporate this interaction by employing one-electron potentials such as conventional functionals. A long-range exchange correction (LRXC) scheme that was supposed by Iikura, Tsuneda and Hirao,[53] was recently applied to the calculations of VdW bond systems.[52] It has been confirmed that this LRXC scheme drastically improves overestimated polarizabilities for π-conjugated polyenes.[53] Dissociation potentials of rare-gas dimers were calculated by combining the LRXC scheme with conventional VdW functionals. Calculated results showed that it gives much more accurate potential energies than usual VdW techniques in DFT, as mentioned in Sec. 2.2.2.

2.1. *Exchange-correlation functional*

2.1.1. *Criteria for the development of functionals*

Most DFT functionals have been developed in accordance with a process that a functional form is assumed on the basis of specific physical conditions, and then is fitted to particular chemical properties with semi-empirical parameters. However, it is inherently preferable that fundamental conditions and accurate properties are given by a functional that is derived from a reasonable physical model with a minimum of adjustable parameters. The customary process may lead to the discharges of functionals that are superior only in a special case. Besides two typical criteria, a functional

(i) obeys the conditions of the exact functional,
(ii) is applicable to a wide class of problems and a wide variety of systems, with the following three criteria to therefore be supplemented,
(iii) is simple with a minimum number of parameters (including fundamental constants),
(iv) contains no additional part for obtaining specific properties, and
(v) has a progressive form that can be updated.[45]

Generalized-gradient-approximation (GGA) correlation functionals, e.g. Perdew–Wang 1991 (PW91)[40] and etc. may conflict with criterion (iii), because some semi-empirical parameters are contained in component LDA correlations; i.e. six parameters in Perdew–Wang functional[54] and four in Vosko–Wilk–Nusair functional.[55] Parameters give rise to spurious wiggles in potentials and lead to an over-complicated functional form.[41] Criterion (iv) is not satisfied by many exchange-correlation functionals that are derived to obey fundamental conditions,[40,41,43] because these conditions also correspond to the specific properties. There may be divergences of opinions to this criterion. It should, however, be noted that additional terms may lead to any functional that satisfies even inconsistent fundamental conditions. The ignorance of criteria (iii) and (iv) seems to lower the reliability of DFT. Finally, criterion (v) is also very important, because it is obvious that a functional will be abandoned in the near future unless it does not satisfy this criterion. It seems reasonable to suppose that we can always develop a functional that is superior to

an inflexible functional. It may also be harmful for the development of DFT that an inflexible functional is used as a *de facto* standard over a long period of time. Based on these five criteria, Pfree exchange and OP correlation functionals are developed.

2.1.2. *Parameter-free exchange functional*

Tsuneda and Hirao developed the analytical parameter-free (Pfree) exchange functional that has neither adjusted parameters nor additional parts.[44] The Pfree exchange functional is given by

$$E_x^{\mathrm{Pfree}} = -\frac{1}{2}\sum_\sigma \int \frac{27\pi}{5\tau_\sigma}\rho_\sigma^3 \left[1 + \frac{7x_\sigma^2\rho_\sigma^{5/3}}{108\tau_\sigma}\right] d^3R \quad (40)$$

where ρ_σ and $\nabla\rho_\sigma$ are the density and the gradient of the density for σ-spin electrons, and x_σ indicates a dimensionless parameter, $x_\sigma = |\nabla\rho_\sigma|/\rho_\sigma^{4/3}$. Kinetic energy density τ_σ is defined in the noninteracting kinetic energy,

$$T_s = \frac{1}{2}\sum_\sigma \int \sum_i^{\mathrm{occ}} |\nabla\psi_{i\sigma}|^2 d^3R = \frac{1}{2}\sum_\sigma \int \tau_\sigma d^3R\,. \quad (41)$$

Equation (40) is derived from the expansion of the spin-polarized Hartree–Fock density matrix up to the second-order,[56–58]

$$P_\sigma\left(R + \frac{r}{2}, R - \frac{r}{2}\right) = \frac{3j_1(k_\sigma r)}{k_\sigma r}\rho_\sigma(R) + \frac{35j_3(k_\sigma r)}{2k_\sigma^3 r} \times \left(\frac{\nabla^2\rho_\sigma(R)}{4} - \tau_\sigma + \frac{3}{5}k_\sigma^2\rho_\sigma(R)\right) \quad (42)$$

where $r = |\mathbf{r}_i - \mathbf{r}_j|, R = (\mathbf{r}_i + \mathbf{r}_j)/2$ and j_n is the nth-order spherical Bessel function. In Eq. (42), k_σ is the averaged relative momentum at each center-of-mass coordinate $\mathbf{R}$, and is reasonably approximated by[44]

$$k_\sigma = \sqrt{\frac{5\tau_\sigma}{3\rho_\sigma}}\,. \quad (43)$$

This k_σ gives the Fermi momentum, $k_\sigma = (6\pi^2\rho_\sigma)^{1/3}$, for the Thomas–Fermi kinetic energy density, $\tau_\sigma = (3/5)(6\pi^2)^{2/3}\rho_\sigma^{5/3}$.

The Pfree exchange functional depends on kinetic energy density τ_σ in Eq. (40) that is adjustable within the applicability of Eq. (42), i.e. for a slowly-varying density. Surprisingly, Pfree exchange functional was proved to give the exact exchange energy in the slowly-varying density limit for the exact τ_σ in this limit.[44] It was also found that Pfree functional estimates atomic exchange energies within an averaged error of about 3% for this τ_σ, despite of the parameter-free form. By adapting various fundamental conditions to the τ_σ, it was confirmed that Pfree functional satisfies all fundamental conditions of exchange functional except for the long-range asymptotic behavior.[59,60] Since Eq. (42) inevitably contains a self-interaction error, it is natural that Pfree exchange does not give the long-range behavior that is dominated by the self-interaction.[61]

2.1.3. *One-parameter progressive correlation functional*

Tsuneda *et al.* also proposed the one-parameter progressive (OP) correlation functional that contains only one parameter and no additional parts,[45,46]

$$E_c^{\mathrm{OP}} = -\int \rho_\alpha\rho_\beta \frac{1.5214\beta_{\alpha\beta} + 0.5764}{\beta_{\alpha\beta}^4 + 1.1284\beta_{\alpha\beta}^3 + 0.3183\beta_{\alpha\beta}^2} \quad (44)$$

where $\beta_{\alpha\beta}$ is given as

$$\beta_{\alpha\beta} = q_{\alpha\beta}\frac{\rho_\alpha^{1/3}\rho_\beta^{1/3}K_\alpha K_\beta}{\rho_\alpha^{1/3}K_\alpha + \rho_\beta^{1/3}K_\beta}\,. \quad (45)$$

In Eq. (45), $q_{\alpha\beta}$ is only one parameter and K_σ is defined in a form of exchange functionals,

$$E_x \equiv -\frac{1}{2}\sum_\sigma \int \rho_\sigma^{4/3}K_\sigma d^3R\,. \quad (46)$$

Equation (44) is derived from the spin-polarized Colle–Salvetti-type correlation wave function for opposite-spin electron pairs,[46,62]

$$\Psi_{\alpha\beta} = \Psi_{\alpha\beta}^0 \prod_{i>j}[1 - \phi_{\alpha\beta}(r_i, r_j)] \quad (47)$$

where r_i is the spatial coordinate of the ith electron and $\Psi_{\alpha\beta}^0$ is a spin-polarized uncorrelated wave function that is multiplied by itself to obtain a spin-polarized uncorrelated second-order reduced density matrix for spin $\alpha\beta$ pairs. The function $\phi_{\alpha\beta}$ satisfies the spin-polarized correlation cusp conditions[63,64] by

$$\phi_{\alpha\beta}(r_i, r_j) = \exp(-\beta_{\alpha\beta}^2 r^2)\left[1 - \left(1 + \frac{r}{2}\right)\Phi_{\alpha\beta}(R)\right] \quad (48)$$

The function $\phi_{\alpha\beta}(R)$ can be described approximately by

$$\Phi_{\alpha\beta} \approx \frac{\sqrt{\pi}\beta_{\alpha\beta}}{\sqrt{\pi}\beta_{\alpha\beta}+1}\,. \tag{49}$$

The parameter $\beta_{\alpha\beta}$ was derived by using Becke's definition of correlation length.[46,65] The only semi-empirical parameter $q_{\alpha\beta}$ is determined for each exchange functional. By applying fundamental conditions of the exact exchange functional to K_σ in Eq. (45), OP correlation functional was surprisingly proved to be the first that satisfies all conditions of the exact correlation functional.[45] Since OP functional has also been numerically backed up by calculations of G2 benchmark set,[45] transition metal dimers,[66,67] and etc. it is now implemented in sophisticated packages of computational chemistry; DMol3,[68] ADF,[69] GAMESS,[70] and so forth.

2.1.4. *Physical connections in molecules*

As mentioned above, Pfree exchange and OP correlation functionals satisfy most fundamental conditions of the exact functionals by adapting conditions of the exact kinetic and exchange functionals to τ_σ in Eq. (40) and K_σ in Eq. (45), respectively.[44,45] Table 4 shows the fundamental conditions and the comparison of exchange-correlation functionals. From the table, it is evident that Pfree + OP (POP) functional satisfies much more conditions than conventional functionals do.[61] We should notice that both Pfree and OP functionals are not derived to obey these conditions. It may indicate that kinetic, exchange, and correlation functionals are transversely connected through Pfree exchange and OP correlation functionals.[47] Only the long-range asymptotic behavior is violated by that Pfree exchange functional, because this behavior is based on the self-interaction of electrons that is not essentially given by GGA functionals.[61]

Molecules obviously contain two kinds of regions where kinetic, exchange, and correlation energies are differently connected; i.e. free-electron and self-interaction regions.[61] In the free-electron region, kinetic, exchange, and correlation energies are well-approximated by gradient approximations and may be transversely connected through Pfree and OP functionals. On the other hand, the self-interaction region comes from the density matrix behavior for self-interacted electron pairs,[71]

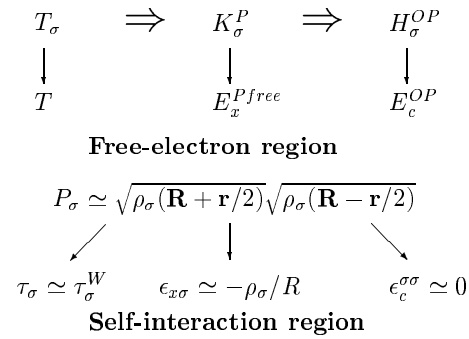

Fig. 7. Physical connections for kinetic, exchange, and correlation energies in free-electron and self-interaction regions. These energies are transversely connected through Pfree and OP functionals in free-electron regions, and are derived from the density matrix behavior in self-interaction regions.

$$P_\sigma\left(R+\frac{r}{2},R-\frac{r}{2}\right) \cong \sqrt{\rho_\sigma\left(R+\frac{r}{2}\right)}\sqrt{\rho_\sigma\left(R-\frac{r}{2}\right)}\,. \tag{50}$$

Based on this behavior, kinetic energy density τ_σ approaches Weizsaecker one,[37]

$$\tau_\sigma^W = \frac{|\nabla\rho_\sigma|^2}{4\rho_\sigma} \tag{51}$$

and exchange energy density $\varepsilon_{x\sigma}$ gives the exact form of hydrogen-like orbitals,[72] as mentioned in the next section. These two physical connections are summarized in Fig. 7.[61] In the figure, T_σ, K_σ^P, and H_σ^{OP} are defined as follows;[47] T_σ is defined using a GGA form of noninteracting kinetic energy,[36]

$$T_s = \frac{1}{2}\sum_\sigma \int \rho_\sigma^{5/3} T_\sigma d^3R\,. \tag{52}$$

Substituting T_σ into Eq. (40) gives K_σ in Eq. (46) for the Pfree exchange functional:

$$K_\sigma^P[x_\sigma,T_\sigma] = \frac{27\pi}{5T_\sigma}\left[1+\frac{7x_\sigma^2}{108T_\sigma}\right]. \tag{53}$$

For K_σ^P, the fractional part of the OP correlation functional in Eq. (44), H_σ^{OP}, is given by

$$H^{\mathrm{OP}}[\beta_{\alpha\beta}P] = \frac{1.5214\beta_{\alpha\beta}+0.5764}{\beta_{\alpha\beta}^4+1.1284\beta_{\alpha\beta}^3+0.3183\beta_{\alpha\beta}^2} \tag{54}$$

where

$$\beta_{\alpha\beta}^P = q_{\alpha\beta}\frac{\rho_\alpha^{1/3}\rho_\beta^{1/3}K_\alpha^P K_\beta^P}{\rho_\alpha^{1/3}K_\alpha^P+\rho_\beta^{1/3}K_\beta^P}\,. \tag{55}$$

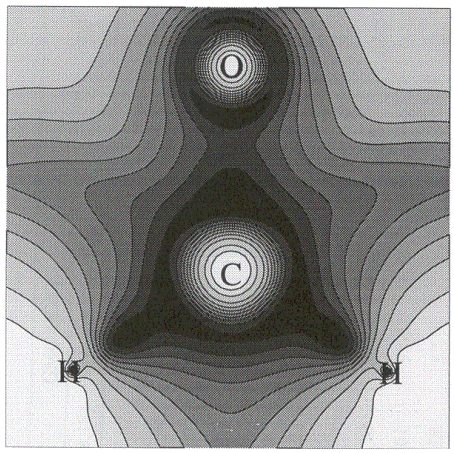

Fig. 8. Contour map of the ratio, $\tau_\sigma^W/\tau_\sigma^{\rm total}$ for formaldehyde molecule. This map reveals self-interaction regions in this molecule.

Where are free-electron and self-interaction regions distributed in molecules? By making use of the relation that total kinetic energy density $\tau_\sigma^{\rm total}$ approaches the Weizsaecker one τ_σ^W in self-interaction regions, the contour map of the ratio, $\tau_\sigma^W/\tau_\sigma^{\rm total}$ can be illustrated, as seen in Fig. 8.[61] The figure shows that self-interaction regions concentrate on near-nucleus and low-density areas, and free-electron regions are conversely distributed around chemical bonds between atoms. In particular, self-interaction regions also dominate around hydrogen atoms. We should notice that DFT tends to underestimate reaction energy barriers especially for reactions where hydrogen atoms take part.[73] It is, therefore, expected that conventional DFT problems may be solved by getting rid of errors from the self-interaction regions of exchange functionals.

2.2. *Correction schemes for exchange functionals*

2.2.1. *Regional self-interaction correction scheme*

Previous DFT calculations have shown that many DFT problems may originate from self-interaction errors. Although various kind of SIC schemes have been suggested so far,[48–50] most conventional SIC schemes intend to take remaining Coulomb self-interactions away, and require much computational timing and considerable efforts for processing orbital-localizations,[49] orbital-dependent transformations,[50] and so forth. Recently, a self-interaction correction (SIC) scheme was proposed to remove self-interaction errors spatiallly from DFT exchange functionals by Tsuneda, Kamiya, and Hirao.[51] Since this scheme simply improves functionals with no additional process mentioned above, it is easily carried out only by solving the Kohn–Sham equation as usual.

In the new SIC scheme, self-interaction regions are identified by making use of the property that total kinetic energy density

$$\tau_\sigma^{\rm total} = \sum_i^{\rm occ} |\nabla\psi_{i\sigma}|^2 \tag{56}$$

where $\psi_{i\sigma}$ is the ith σ-spin molecular orbital, approaches the Weizsaecker one for self-interacted electrons.[37] That is, it is supposed that self-interaction regions correspond to the areas where index t_σ,

$$t_\sigma = \frac{\tau_\sigma^W}{\tau_\sigma^{\rm total}}\,(0 < t_\sigma \le 1) \tag{57}$$

approaches 1.

Self-interacted electrons may have hydrogen-like atomic orbitals,

$$\psi_\sigma = \sqrt{\frac{\alpha^3}{\pi}}\,\exp(-\alpha R) \tag{58}$$

because $\tau_\sigma^{\rm total}$ is proved to coincide with the Weizsaecker one for such orbitals. It is easily proved for such orbitals that the exchange self-interaction energy density corresponds to the exact one,

$$\varepsilon_{x\sigma}^{\rm SIC}(R) = -\frac{\rho_\sigma}{R}[1 - (1+\alpha R)\exp(-2\alpha R)] \tag{59}$$

where $\varepsilon_{x\sigma}$ is defined by $E_x = \sum_\sigma \int \varepsilon_{x\sigma} d^3R$. Based on Eq. (57), the exponent α is easily obtained by

$$\alpha = \frac{|\nabla\rho_\sigma|}{2\rho_\sigma} \tag{60}$$

because density $\rho\sigma$ is expressed by $\rho_\sigma = |\psi_\sigma|^2$ in self-interaction regions.

To make use of Eq. (57), a partition function is necessary to cut self-interaction regions out from the molecule. For this purpose, partition function f_σ was employed,

$$f_\sigma = \frac{1}{2}\left(1 + {\rm erf}\left[\frac{5(t_\sigma - a)}{1-a}\right]\right)(0 < a < 1) \tag{61}$$

where a is a parameter that corresponds to the boundary point. By using f_σ, exchange energy densities are

smoothly divided into the free-electron part (i.e. t_σ is apart from 1) that is correctly approximated by conventional exchange functionals and the self-interaction part (i.e. t_σ is close to 1) that is exactly given by Eq. (59), such that

$$\varepsilon_{x\sigma}(R) = f_\sigma \varepsilon_{x\sigma}^{\mathrm{SIC}}(R) + (1 - f_\sigma)\varepsilon_{x\sigma}^{\mathrm{DFT}}(R)\,. \qquad (62)$$

The regional SIC scheme was applied to energy diagram calculations of the $H_2CO \rightarrow H_2 + CO$ reaction.[51] DFT studies have reported that conventional exchange-correlation functionals underestimate the energy barrier of this reaction by a few kcal mol^{-1} in comparison with experimental results. Unrestricted Kohn–Sham calculations were carried out using cc-pVQZ basis functions[23] with $96 \times 12 \times 24$-point prune grids. Becke exchange + OP correlation (BOP) functional[45] was employed, and zero-point vibrational correction was taken into account. As a result, it was found that the reaction barrier energy (Exp. 79 kcal mol^{-1}) was obviously improved from 72 kcal mol^{-1} to 82 kcal mol^{-1} before and after SIC. This value is mostly equivalent to the result of *ab initio* CCSD(T) scheme.[51] As far as we know, this may be the first SIC scheme that gets rid of the self-interaction error as a correction to functionals.

2.2.2. *Long-range exchange correction scheme*

As mentioned above, most DFT problems have been reported to originate from self-interaction errors. In exchange-correlation functionals, there are, however, some problems that may not be interpreted by SIE. The most remarkable example may be the difficulty of Van der Waal's (VdW) calculations. As far as we know, accurate VdW bonds of rare-gas dimers are inclusively given by neither functionals nor correction schemes in DFT.[52] This failure has been attributed to the lack of VdW interactions in conventional correlation functionals. It is, however, reported that VdW bonds are not reproduced by incorporating VdW interactions in conventional functionals.[52] On the hypothesis that this may be due to the lack of the long-range exchange interaction in exchange functionals, the long-range exchange correction (LRXC) scheme for exchange functionals[53] was applied to VdW calculations by combining with a VdW functional.

In the LRXC scheme developed by Iikura, Tsuneda and Hirao,[53] the two-electron operator $1/r_{12}$ is separated into the short-range and long-range parts naturally by using the standard error function erf such that[74,75]

$$\frac{1}{r_{12}} = \frac{1 - \mathrm{erf}(\mu r_{12})}{r_{12}} + \frac{\mathrm{erf}(\mu r_{12})}{r_{12}} \qquad (63)$$

where μ is a parameter that determines the ratio of these parts. The long-range exchange interaction is described by the Hartree–Fock exchange integral,[76]

$$E_x^{lr} = -\frac{1}{2}\sum_\sigma \sum_i^{\mathrm{occ}} \sum_j^{\mathrm{occ}} \iint d^3r_1 d^3r_2 \psi_{i\sigma}^*(r_1)\psi_{j\sigma}^*(r_2) \times \frac{\mathrm{erf}(\mu r_{12})}{r_{12}} \psi_{j\sigma}(r_1)\psi_{i\sigma}(r_2) \qquad (64)$$

and an exchange functional is applied to the short-range part such that[74]

$$E_x^{sr} \equiv -\frac{1}{2}\sum_\sigma \int \rho_\sigma^{4/3} K_\sigma \left(1 - \frac{8}{3}a_\sigma \left[\sqrt{\pi}\,\mathrm{erf}\left(\frac{1}{2a_\sigma}\right) + (2a_\sigma - 4a_\sigma^3)\exp\left(-\frac{1}{4a_\sigma^2}\right) - 3a_\sigma + 4a_\sigma^3\right]\right) d^3R \qquad (65)$$

where $a_\sigma = \mu/(2k_\sigma)$ and K_σ is defined in Eq. (46). The averaged relative momentum k_σ is given by[53]

$$k_\sigma = \left(\frac{9\pi}{K_\sigma}\right)^{1/2} \rho_\sigma^{1/3} \qquad (66)$$

that reproduces the Fermi momentum, i.e. $k_{F\sigma} = (6\pi^2\rho_\sigma)^{1/3}$, for K_σ of the local spin density approximation exchange functional, $K_\sigma = 3(3/4/\pi)^{1/3}$. It is reported that this LRXC scheme improves underestimated $4s$–$3d$ interconfigurational energies (ICEs) of the first-row transition metal dimers and overestimated longitudinal polarizabilities (LPs) of π-conjugated polymer chains compared to those of usual DFTs.

The LRXC scheme was applied to potential energy calculations of rare-gas dimmers with a VdW functional by Kamiya, Tsuneda and Hirao.[52] In this study, it was postulated that VdW bonds are formed under the balance of VdW and long-range exchange interactions. As the VdW functional, Andersson–Langreth–Lundqvist (ALL) VdW functional,[77]

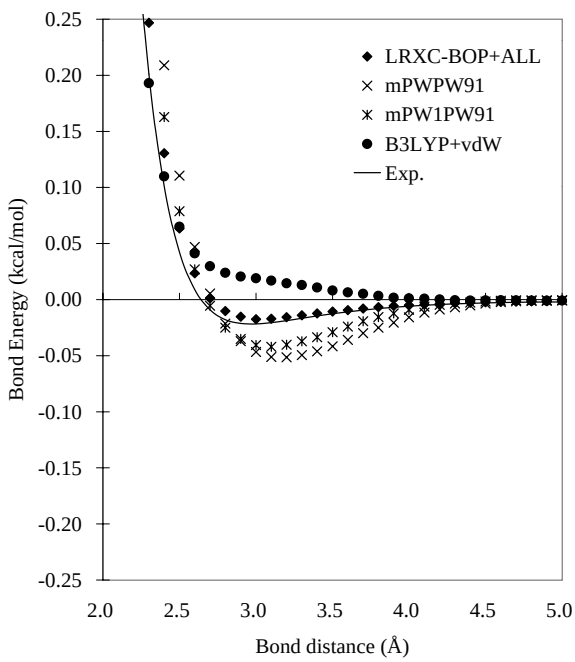

(a) He_2

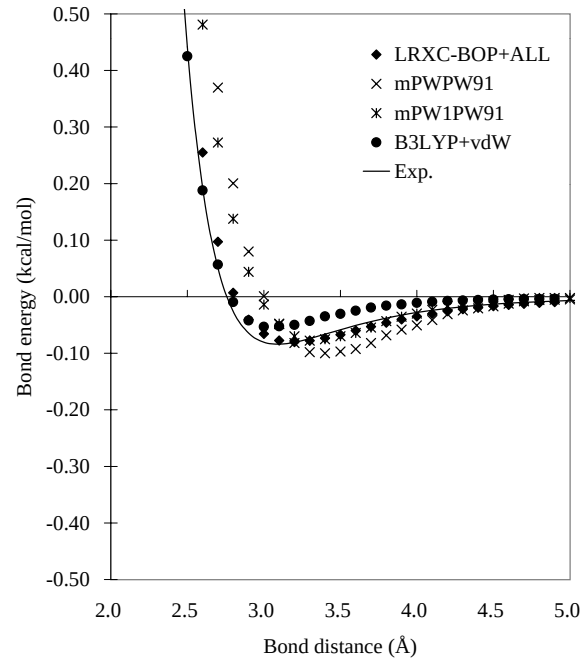

(b) Ne_2

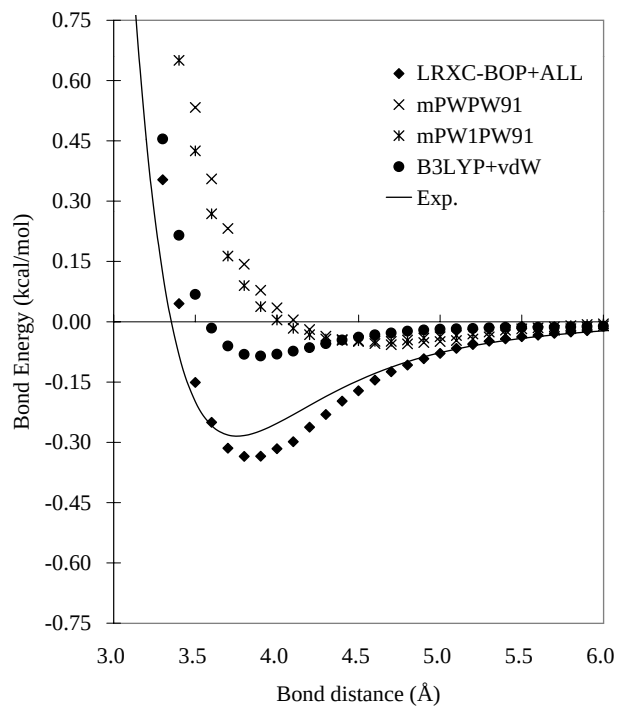

(c) Ar_2

Fig. 9. Calculated dissociation potential energies of He_2, Ne_2, and Ar_2 molecules in hartree.

$$E_c^{\mathrm{VdW}} = -\frac{3}{2(4\pi)^{3/2}} \int_{V_1} d^3r_1 \int_{V_2} d^3r_2 \times \frac{\sqrt{\rho_1(r_1)\rho_2(r_2)}}{\sqrt{\rho_1(r_1)} + \sqrt{\rho_2(r_2)}} \frac{1}{|r_1 - r_2|^6} \quad (67)$$

was employed. It is proved that the ALL functional correctly behaves in either detached harmonic electron gases or separated atoms. An exponential form,

$$f_{\mathrm{damp}} = \exp\left(-\frac{a^6}{|r_1 - r_2|^6}\right) \quad (68)$$

was employed as the damping factor for short-range electron–electron interactions,[52] The 6-311++ $G(3df, 3pd)$ basis functions[78–80] were used with 96-point Euler–Maclaurin quadrature for radial grids and 36×72-point Gauss–Legendre quadrature for angular grids. BOP functional[45] was employed as the exchange-correlation functional. Basis set superposition error was corrected by a counterpoise method.[81] For comparison, mPWPW91,[82] mPW1PW91,[82] and hybrid B3LYP with VdW correction (B3LYP+VdW)[82] schemes were also calculated.

Calculated potential energy curves of He_2, Ne_2, Ar_2 are shown in Fig. 9.[52] Compared with conventional DFTs, it is found that all VdW potentials are dramatically improved by introducing the LRXC scheme, while other schemes give poor potentials especially for He_2 and Ar_2. We should notice that the LRXC scheme contains no parameters depending on calculated atoms. It was, therefore, established that the long-range exchange interactions must be incorporated to give accurate VdW bonds by DFT besides VdW interactions.

3. Relativistic Effect

Since heavy-element systems are involved in many important chemical and physical phenomena, many theoretical and experimental chemists are interested in the investigation of so-called "heavy atom" effects. The relativistic effect underlying in such heavy atoms had not been regarded as an important effect for chemical properties because most chemists thought that the relativistic effects appear primarily in the core electrons. Recent studies, however, have revealed the importance of the relativistic effects, which play essential and vital roles in total natures of molecular electronic structures for heavy-element systems.

In order to treat the relativistic effect theoretically, the Dirac equation is solved instead of the non-relativistic Schrödinger equation. The Dirac equation has the following one-particle Hamiltonian,

$$h_D = c\boldsymbol{\alpha} \cdot \mathbf{p}(\boldsymbol{\beta} - 1)c^2 + V(\mathbf{r}) \quad (69)$$

where the constant c is the speed of light, $V(\mathbf{r})$ is the external potential, and $\mathbf{p}(= -i\nabla)$ is the momentum operator. The 4×4 Dirac matrices $\boldsymbol{\alpha}$ and $\boldsymbol{\beta}$ in Eq. (69) are given by

$$\alpha_t \equiv \begin{pmatrix} 0_2 & \sigma_t \\ \sigma_t & 0_2 \end{pmatrix}, \qquad t = (x, y, z),$$
$$\boldsymbol{\beta} \equiv \begin{pmatrix} \mathbf{I}_2 & 0_2 \\ 0_2 & -\mathbf{I}_2 \end{pmatrix} \quad (70)$$

with 2×2 Pauli spin matrix, σ_t,

$$\sigma_x \equiv \begin{pmatrix} 0 & 1 \\ 1 & 0 \end{pmatrix}, \qquad \sigma_y \equiv \begin{pmatrix} 0 & -i \\ i & 0 \end{pmatrix},$$
$$\sigma_z \equiv \begin{pmatrix} 1 & 0 \\ 0 & -1 \end{pmatrix}. \quad (71)$$

The Dirac Hamiltonian provides a physical structure that the eigenvalue spectrum $\{E_k\}$ consists of two parts. The higher-energy spectrum, where $E_k \geq mc^2$, are called the positive state and comprises states corresponding to those found in non-relativistic theory. The second branch of the eigenvalue spectrum consists of states with energy less than $-mc^2$, and in a second-quantized theory they can be interpreted as states of positrons and are called the negative state.

Since the Dirac equation is valid only for the one-particle system, we have to extend the one-particle Dirac equation and its Hamiltonian to the many-particle systems. The straightforward way to apply the Dirac equation to the many-particle systems is that the one-particle Dirac operator is augmented by the Coulomb or Breit (or approximated Gaunt) operator as the two-particle term, g_{ij}, to produce the Dirac–Coulomb (DC) or Dirac–Coulomb–Breit (DCB) Hamiltonian derived from quantum electrodynamics (QED),

$$H = \sum_i h_D(\mathbf{r}_i) + \sum_{i>j} g_{ij} \quad (72)$$

where

$$g_{ij}^{C} = \frac{1}{r_{ij}} \tag{73}$$

or

$$g_{ij}^{\mathrm{CB}} = \frac{1}{r_{ij}} - \frac{1}{2}\left(\frac{(\alpha_i \cdot \alpha_j)}{r_{ij}} + \frac{(\alpha_i \cdot r_{ij})(\alpha_j \cdot r_{ij})}{r_{ij}^3}\right). \tag{74}$$

In the following sections, we will survey the efficient relativistic electronic structure theories to treat heavy-atomic molecular systems accurately via the four-component and the two-component relativistic approaches. We firstly introduce the four-component Dirac–Hartree–Fock and Dirac–Kohn–Sham methods over the kinetically balanced Gaussian-type spinors.

Our two-component quasi-relativistic developments, RESC and higher-order Douglas–Kroll (DK) Hamiltonians, are introduced in the sequential section. As another review for our recent development of the relativistic electronic structure theories, see Ref. 84.

3.1. *Four-component relativistic approach*

3.1.1. *Dirac–Hartree–Fock and Dirac–Kohn–Sham approaches*

The Dirac–Hartree–Fock (DHF) equation is one of the starting equations employing the many-particle relativistic Hamiltonian. By applying the independent particle approximation to many-particle relativistic Hamiltonians such as DC or DCB Hamiltonians, like a procedure for the non-relativistic Hartree–Fock theory, we can obtain the four-component DHF method with large- and small-component spinors treated explicitly.

The DHF wave function Ψ is given as the following Slater determinant with N^{elec} one-particle spinors $\{\psi_i(\mathbf{r}_\lambda), i = 1, \ldots, N^{\mathrm{elec}}\}$, where N^{elec} represents the number of electrons. The one-particle spinor $\psi_i(\mathbf{r}_\lambda)$ is the four-component vector, whose components are the scalar wave functions,

$$\psi_i = \begin{pmatrix} \psi^{2L} \\ \psi_i^{2S} \end{pmatrix} = \begin{pmatrix} \psi_{1i}^{L} \\ \psi_{2i}^{L} \\ \psi_{3i}^{S} \\ \psi_{4i}^{S} \end{pmatrix}. \tag{75}$$

The two-component vectors ψ_i^{2L} and ψ_i^{2S} are called as the large-component and small-component spinors, respectively, which are expanded in the basis spinors φ^L and φ^S.

The matrix DHF equation is given as

$$\mathbf{Fc} = \mathbf{Sc}\boldsymbol{\varepsilon} \tag{76}$$

where $\mathbf{c}$ is a matrix of molecular spinor coefficients, $\boldsymbol{\varepsilon}$ is a diagonal spinor energy matrix, $\mathbf{S}$ is an overlap matrix,

$$\mathbf{S}_{pq} = \begin{pmatrix} \langle \varphi_p^L | \varphi_q^L \rangle & 0 \\ 0 & \langle \varphi_p^S | \varphi_q^S \rangle \end{pmatrix} \tag{77}$$

and the Fock matrix $\mathbf{F}$ is given by

$$\mathbf{F}_{pq} = \begin{pmatrix} \mathbf{V}^{LL} + \mathbf{J}_{pq}^{LL} - \mathbf{K}_{pq}^{LL} & c\Pi_{pq}^{LS} - \mathbf{K}_{pq}^{LS} \\ c\Pi_{pq}^{SL} - \mathbf{K}_{pq}^{SL} & \mathbf{V}_{pq}^{SS} + \mathbf{J}_{pq}^{SS} - \mathbf{K}_{pq}^{SS} - 2c^2\mathbf{S}_{pq}^{SS} \end{pmatrix}. \tag{78}$$

The matrices $\Pi_{pq}^{X\bar{X}}$, $\mathbf{V}_{pq}^{XX}$, $\mathbf{J}_{pq}^{XX}$, and $\mathbf{K}_{pq}^{XY}$ $(X, Y = L$ or S, $\bar{L} = S$, and $\bar{S} = L)$ are the kinetic energy integral, the nuclear attraction integral, the Coulomb integral, and the exchange integral, respectively, defined by

$$\Pi_{pq}^{X\bar{X}} = \langle \varphi_p^X | (\boldsymbol{\sigma} \cdot \mathbf{p}) | \varphi_q^{\bar{X}} \rangle \tag{79}$$

$$\mathbf{V}_{pq}^{XX} = \langle \varphi_p^X | V^{\mathrm{nuc}} | \varphi_q^X \rangle \tag{80}$$

$$\mathbf{J}_{pq}^{XX} = \sum_{Y=L,S} \sum_{r,s} \mathbf{P}_{sr}^{YY} (\varphi_p^{2X} \varphi_q^{2X} | \varphi_r^{2Y} \varphi_s^{2Y}) \tag{81}$$

and

$$\mathbf{K}_{pq}^{XY} = \sum_{r,s} \mathbf{P}_{sr}^{XY} (\varphi_p^{2X} \varphi_s^{2X} | \varphi_r^{2Y} \varphi_q^{2Y}). \tag{82}$$

The matrix $\mathbf{P}_{sr}^{XY}$ is the density matrix calculated as

$$\mathbf{P}_{sr}^{XY} = \sum_{a}^{N^{\mathrm{elec}}} c_{sa}^{X} c_{ra}^{Y^*} \tag{83}$$

where negative energy states are ignored. The total electronic energy is

$$E^{\mathrm{DHF}} = \frac{1}{2}\{\mathrm{tr}(\mathbf{Ph}^{\mathrm{core}}) + \mathrm{tr}\{\mathbf{PF}^{\mathrm{DC}})\} \tag{84}$$

where $\mathbf{h}^{\mathrm{core}}$ is the bare core Hamiltonian matrix.

The calculation with the chemical accuracy in the heavy-element system requires the incorporation of both relativistic and electron correlation effects. A density functional theory (DFT) offers an attractive alternative for including correlation effects

in calculations on ground-state molecular properties. This theory gives reliable accuracy and is generally computationally less demanding than conventional electron-correlation approaches. While DFT has been extensively applied to nonrelativistic calculations, the four-component DFT approaches have recently appeared. Relativistic DFT was formulated by Rajagopal and Callaway[85] as a generalization of the Hohenberg–Kohn–Sham theory of the inhomogeneous electron gas. The corresponding four-component Dirac–Kohn–Sham (DKS) equation has been derived from QED by Rajagopal[86] and MacDonald and Vosko.[87] Within the no-sea approximation to the relativistic Kohn–Sham equations, Varga *et al.*[88] have performed four-component molecular DFT calculations of the total energy and its gradient with the RLDA and RGGA functionals by employing a numerical basis set. Another numerical four-component DFT program has been developed and successfully applied by Liu *et al.*[89] They employed a frozen core approximation and four-component basis expansion for the valence spinors, which were a combination of numerical atomic spinors and Slater-type functions.

The one-electron effective Hamiltonian for the DKS derived from QED takes the form,

$$h_{\mathrm{DKS}} = h_D + \nu_H + \nu_{\mathrm{xc}} \tag{85}$$

where h_D is the one-electron Dirac operator of Eq. (69), and the ν_H is the Hartree potential,

$$\nu_H = \int \frac{\rho(\mathrm{r}')}{|\mathbf{r} - \mathbf{r}'|} d\mathbf{r}' \tag{86}$$

where $\rho(\mathbf{r})$ is the charge density and ν_{xc} is the exchange-correlation potential. ν_{xc} is the functional derivative of the exchange-correlation energy functional with respect to the density ρ,

$$\nu_{\mathrm{xc}} = \frac{\delta E_{\mathrm{xc}}[\rho]}{\delta \rho} \,. \tag{87}$$

The density $\rho(\mathbf{r})$ is expressed approximately in terms of a set of auxiliary occupied one-electron spinors as

$$\rho(\mathbf{r}) = \sum_i^{N^{\mathrm{elec}}} |\psi_i(\mathbf{r})|^2 \tag{88}$$

where positron states are ignored by employing the no-sea approximation. The DKS equation is then the matrix pseudoeigenvalue equation by introducing basis set expansion as

$$\mathbf{h}^{\mathrm{DKS}}\mathbf{c} = \mathbf{S}\mathbf{c}\boldsymbol{\varepsilon} \tag{89}$$

where $\mathbf{h}^{\mathrm{DKS}}$ takes the form of a Fock matrix,

$$\mathbf{h}^{\mathrm{DKS}}_{pq} = \begin{pmatrix} \mathbf{V}^{LL}_{pq} + \mathbf{J}^{LL}_{pq} - \mathbf{v}^{LL}_{\mathrm{xc}pq} & c\Pi^{LS}_{pq} \\ c\Pi^{SL}_{pq} & \mathbf{V}^{SS}_{pq} + \mathbf{J}^{SS}_{pq} - \mathbf{v}^{SS}_{\mathrm{xc}pq} - 2c^2\mathbf{S}^{SS}_{pq} \end{pmatrix} \tag{90}$$

where $\mathbf{v}^{XX}_{\mathrm{xc}pq}$ is the exchange-correlation potential defined by

$$\mathbf{v}^{XX}_{\mathrm{xc}pq} = \left\langle \varphi^X_p \left| \frac{\delta E_{\mathrm{xc}}}{\delta \rho} \right| \varphi^X_q \right\rangle . \tag{91}$$

The total electronic energy is

$$E^{\mathrm{DKS}} = \frac{1}{2}\mathrm{tr}(\mathbf{P}\mathbf{h}^{\mathrm{core}}) + \frac{1}{2}\mathrm{tr}\{\mathbf{P}(\mathbf{h}^{\mathrm{DKS}} + \mathbf{v}_{\mathrm{xc}})\} + E_{\mathrm{xc}}[\rho] \,. \tag{92}$$

3.1.2. *Efficient computational scheme for DHF and DKS methods*

The DHF or DKS method with the four-component spinors is a theoretically simple and straightforward approach. Although several four-component *ab initio* molecular orbital programs for polyatomics, MOLFDIR,[90] DIRAC[91] and BERTHA[92] and others have been developed in the last decade, the treatment of more than one heavy atoms within a molecule is not yet routine. The main bottleneck in four-component calculations on heavy-element systems is an evaluation of the two-electron AO integrals. The difficulty in introducing contracted Gaussian-type spinors (GTSs) lies in the fact that the kinetic balance condition between the large- and small-component primitive GTSs must be incorporated.

Recently, we presented a highly efficient computational scheme for the four-component method as a step toward routine fully relativistic calculations on molecules containing more than one or two heavy atoms. In this review, we briefly introduce our computational scheme because the details are given in Refs. 93–95. Our fully relativistic density functional

method is the first implementation for the Gaussian-based DKS method.

We adopt the spin-coupled generally contracted Gaussian-type spinors as the basis. Thus the basis expansion is expressed as

$$\begin{pmatrix} \psi_i^{2L} \\ \psi_i^{2S} \end{pmatrix} = \sum_{\mu}^{n} \begin{pmatrix} c_{\mu i}^{L}\ \varphi_{\mu}^{2L} \\ c_{\mu i}^{S}\ \varphi_{\mu}^{2S} \end{pmatrix} \tag{93}$$

where the basis spinors φ_μ^{2L} and φ_μ^{2S} are two-component basis spinors, and the expansion coefficients c_μ^L and c_μ^S are scalar variables. In Eq. (93), two scalar wave functions within a two-component basis spinor are multiplied by a common expansion coefficient, the dimensions of both the large and small components are n, and the total number of variational parameters, consequently, is $2n$. In contrast to the pioneering four-component program package MOLFDIR, our scheme requires fewer functions in the small component. This efficiency works to reduce the computational demands effectively for storage, computation, and transformation of integrals.

The form of the basis spinors is determined by the linear combination of atomic orbitals (LCAO) approach. While the spinors of the analytical solution include Slater-type functions, they are replaced by Gaussian-type functions for the sake of computational efficiency. First, assume the two-component basis spinors to be generally contracted spherical harmonic Gaussian-type spinors (GTSs),

$$\varphi_\mu^{2L} = \sum_{k}^{K} d_{k\mu}^{L} \phi_K^{2L} \tag{94}$$

$$\varphi_\mu^{2S} = \sum_{k}^{K} d_{k\mu}^{S} \phi_k^{2S} \tag{95}$$

where ϕ_k^{2L} and ϕ_k^{2S} are primitive spherical harmonic GTSs containing a common orbital exponent, $d_{k\mu}^L$ and $d_{k\mu}^S$ are the contraction coefficients, and K is the degree of contraction. The contraction coefficients $d_{k\mu}^L$ and $d_{k\mu}^S$ should be treated separately for large and small components, because separate atomic orbital (AO) coefficients for the large and small components are obtained from a four-component atomic calculation.

The form of the large-component primitive GTS ϕ_k^{2L} is chosen from the large-component spinors obtained by analytical solution of the one-electron Dirac equation. The small-component primitive GTS ϕ_k^{2S} is given analytically in order that it may satisfy the kinetic balance condition[96] versus the corresponding large-component primitive GTS ϕ_k^{2L},

$$\phi_k^{2S} = i(\boldsymbol{\sigma} \cdot \mathbf{p}) \phi_k^{2L} \,. \tag{96}$$

This condition avoids the condition known as 'variational collapse'.

In our contraction scheme, the contracted GTSs no longer obey Eq. (96), but rather the more accurate relation,

$$\phi_k^{2S} = i(V - E - 2c^2)^{-1} (\boldsymbol{\sigma} \cdot \mathbf{p}) \phi_k^{2L} \,. \tag{97}$$

We note that a contraction scheme such as that used in MOLFDIR cannot satisfy Eq. (97) exactly.

Most of the previous DHF programs[90–92] employ extant non-relativistic quantum chemistry algorithms to evaluate the elements of the DHF matrix in a scalar Gaussian basis. In their implementations, the structure of four-component Dirac spinors is ignored. Molecular four-component spinors are expanded in decoupled scalar spin-orbitals, making the implementation of molecular double group symmetry in one- and two-electron integrals difficult. Our algorithms retain the structure of atomic spinors to exploit molecular double group symmetry in generating integrals. Four-component molecular spinors are expanded in basis sets of generally contracted spherical harmonic Gaussian-type two-component spinors.

In our scheme, relativistic AO integrals are estimated via the fast non-relativistic electron repulsion integral (ERI) routine SPHERICA, which is a highly efficient algorithm for calculating ERIs that we have developed and implemented.[97] The algorithm is based on the ACE-b3k3 formula[98] with the general contraction. Because the bulk of relativistic effects is the kinematic effects coming from the core region, it is important to employ a large number of basis functions especially in the core and to contract them for computational efficiency. Our strategy for generating integrals efficiently is to express the integrals in generally contracted spherical harmonic GTSs, which are in turn expressed in generally contracted spherical harmonic Gaussian-type orbitals (GTOs) so as to exploit highly efficient SPHERICA algorithm.

The several numerical results show the efficiency in our algorithm. The details are given in original Refs. 93–95.

3.2. *Two-component quasi-relativistic approach*

Despite our implementation of the efficient algorithm for the four-component relativistic approach, the Dirac–Coulomb(–Breit) equation with the four-component spinors composed of the large (upper) and small (lower) components demands severe computational efforts to solve now still, and its applications to molecules are limited to small- and medium-size systems currently. Thus, several two-component quasi-relativistic approximations are applied to the chemically interesting systems including heavy elements instead of explicitly solving the four-component relativistic Dirac equation.

The Breit–Pauli (BP) approximation[99] is obtained truncating the Taylor expansion of the Foldy–Wouthuysen (FW) transformed Dirac Hamiltonian[100] up to the $(p/mc)^2$ term. The BP equation has the well-known mass-velocity, Darwin, and spin-orbit operators. Although the BP equation gives reasonable results in the first-order perturbation calculation, it cannot be used in the variational treatment.

One of the shortcomings of the BP approach is that the expansion in $(p/mc)^2$ is not justified in the case where the electronic momentum is too large, e.g. for a Coulomb-like potential. The zeroth-order regular approximation (ZORA) [101] can avoid this disadvantage by expanding in $E/(2mc^2 - V)$ up to the first order. The ZORA Hamiltonian is variationally stable. However, the Hamiltonian obtained by a higher-order expansion has to be treated perturbatively, similarly to the BP Hamiltonian.

Recently, we have developed two quasi-relativistic approaches; one is the RESC method[102] and another is the higher-order Douglas–Kroll method.[103] In this section, we will review these theories briefly.

3.2.1. *RESC method*

The Dirac equation has the four-component spinors,

$$\Psi = \begin{pmatrix} \Phi^L \\ \Phi^S \end{pmatrix} \tag{98}$$

where Ψ^L and Φ^S are the large (upper) and small (lower) components, respectively. The Dirac spinor Ψ is normalized as

$$\langle \Psi | \Psi \rangle = \langle \Psi^L | \Psi^L \rangle + \langle \Psi^S | \Psi^S \rangle = 1 \tag{99}$$

while neither Ψ^L nor Ψ^S is normalized. The Dirac equation, Eq. (69), can be written as coupled equations,

$$V\Psi^L + c(\boldsymbol{\sigma} \cdot \mathbf{p})\Psi^S = E\Psi^L \tag{100a}$$

$$c(\boldsymbol{\sigma} \cdot \mathbf{p})\Psi^L + (V - E - 2mc^2)\Psi^S = 0 \tag{100b}$$

where $\boldsymbol{\sigma}$ stands for the 2×2 Pauli spin matrix vector. From Eq. (100b), the small component is expressed as

$$\Psi^S = [2mc^2 - (V - E)]^{-1} c(\boldsymbol{\sigma} \cdot \mathbf{p})\Psi^L \equiv X\Psi^L \,. \tag{101}$$

By substitution of this equation into Eq. (100a), the Schrödinger–Pauli type equation composed of only the large component is obtained as

$$\left[V + (\boldsymbol{\sigma} \cdot \mathbf{p}) \frac{c^2}{2mc^2 - (V - E)} (\boldsymbol{\sigma} \cdot \mathbf{p}) \right] \Psi^L = E\Psi^L \,, \tag{102a}$$

and the normalization condition, Eq. (99) becomes

$$\langle \Psi^L | 1 + X^+ X | \Psi^L \rangle = 1 \,. \tag{102b}$$

Note that no approximation has been made so far. If we can solve Eq. (102a) with Eq. (102b), the Dirac solution can be obtained exactly.

However, it is difficult to solve this equation since Eq. (102) has the energy and the potential in the denominator. An appropriate approximation has to be introduced. In our strategy, $E - V$ in the denominator is replaced by *the classical relativistic kinetic energy* (relativistic substitutive correction),

$$T = (m^2c^4 + p^2c^2)^{1/2} - mc^2 \,. \tag{103}$$

The idea is simple and straightforward. This approach is referred to as the relativistic scheme by eliminating small components (RESC). The derivation of this approach is given in Ref. 102. The resulting RESC Hamiltonian H_{RESC} can be separated into the spin-free (sf) and spin-dependent (sd) parts as

$$H_{\mathrm{RESC}} = H^{sf}_{\mathrm{RESC}} + H^{sd}_{\mathrm{RESC}} \tag{104}$$

where

$$H^{sf}_{\mathrm{RESC}} = T + OQ\mathbf{q} \cdot V\mathbf{p}QO^{-1} + 2mcOQ^{1/2}VQ^{1/2}O^{-1} \tag{105}$$

and

$$H^{sd}_{\mathrm{RESC}} = iOQ\boldsymbol{\sigma}\cdot(\mathbf{p}V)\times\mathbf{p}QO^{-1}\,. \tag{106}$$

Here, O and Q operators are defined by

$$O = \frac{1}{E_p + mc^2}\left(1 + \frac{p^2c^2}{(E_p + mc^2)}\right)^{1/2} \tag{107}$$

and

$$Q = \frac{c}{E_p + mc^2} \tag{108}$$

where

$$E_p = (p^2c^2 + m^2c^4)^{1/2}\,. \tag{109}$$

Although we have so far treated one-electron equation, the resulting equation can be easily extended to the many-electron case. For a practical calculation, the Hamiltonian matrix elements are evaluated in the space spanned by the eigenfunctions of the square momentum p^2 following Buenker and Hess,[104] as well as the Douglas–Kroll–Hess (DKH) approach.[105] H_{RESC} is symmetrized to be Hermitian for mathematical convenience, instead of the physical significance.

The RESC approach has several advantages. It is variationally stable. This method can easily be implemented in various non-relativistic *ab initio* programs, and the relativistic effect is considered on the same footing with the electron correlation effect. The RESC approach has been applied to various systems in ground and excited states.[106–113] RESC has been known to work well for a number of systems, and recent studies show that RESC gives similar results for the chemical properties as the DKH method, although very large exponents in the basis set can lead to variational collapse in a current RESC approximation, partly because the current implementation includes only the lowest truncation of the O operator. Since the energy gradient of the RESC method is also available currently,[114] we can study the chemical reaction in the heavy element systems.

3.2.2. *Higher-order Douglas–Kroll method*

The Douglas–Kroll (DK) transformation[115] can decouple the large and small components of the Dirac spinors in the presence of an external potential by repeating several unitary transformations. The DK transformation is a variant of the Foldy–Wouthuysen (FW) transformation,[100] with an alternative natural expansion parameter, the external potential V_{ext} (or the coupling strength Ze^2), and avoids the high singularity in the FW transformation.

The first step in the DK transformation consists of a free-particle FW transformation in momentum space. Using the free-particle eigensolutions of the Dirac Hamiltonian associated with the positive energy eigenvalues, the unitary operator in the free-particle FW transformation is given as

$$U_0 = A(1 + \beta R) \tag{110}$$

where A and R are operators defined by

$$A = \left(\frac{E_p + c^2}{2E_p}\right)^{1/2} \tag{111}$$

$$R = \frac{c\boldsymbol{\alpha}\cdot\mathbf{p}}{E_p + c^2}\,. \tag{112}$$

Application of this unitary operator to the Dirac Hamiltonian in the external field, H_D^{ext}, gives

$$\begin{aligned} H_1 &= U_0 H_D^{\mathrm{ext}} U_0^{-1} \\ &= \beta E_p + E_1 + O_1 \end{aligned} \tag{113}$$

where E_1 and O_1 are the even and odd operators of first order in the external potential, respectively,

$$E_1 = A(V_{\mathrm{ext}} + RV_{\mathrm{ext}}R)A \tag{114}$$

$$O_1 = \beta A(RV_{\mathrm{ext}} - V_{\mathrm{ext}}R)A\,. \tag{115}$$

Douglas and Kroll suggested that it is possible to remove odd terms of arbitrary orders in the external potential through successive unitary transformations

$$U_n = (1 + W_n^2)^{1/2} + W_n \tag{116}$$

where W_n is an anti-Hermitian operator of order V_{ext}^n. Alternatively, we introduce an exponential-type unitary operator of the form,[103]

$$U_n = \exp(W_n)\,. \tag{117}$$

The essence of the DK transformation is to remove odd terms by repeating *arbitrary* unitary transformations. Expanding Eqs. (116) and (117) in a power series of W_n, we note that both expansions are common up to second order. One should note that an exponential-type unitary operator, instead of a conventional form, is used in order to derive the

higher-order DK Hamiltonians easily, since the exponential-type operator can take full advantage of the Baker–Cambell–Hausdorff expansion.

The $2n+1$ rule also simplifies the formulations of the high-order DK Hamiltonians significantly.[103] The $2n+1$ rule reads that generally the anti-Hermitian W_n of order $V_{\rm ext}^n$ determines the DK Hamiltonian (or its energy) to order $2n+1$.

The resulting nth-order DK (DKn) Hamiltonians[103] are given as

$$H_{\rm DK2} = \beta E_p + E_1 - \frac{1}{2}[W_1[W_1, \beta E_p]] \tag{118}$$

$$H_{\rm DK3} = H_{\rm DK2} + \frac{1}{2}[W_1, [W_1, E_1]] \tag{119}$$

$$H_{\rm DK4} = H_{\rm DK3} - \frac{1}{8}[W_1, [W_1, [W_1, [W_1, \beta E_p]]]] + [W_2, [W_1, E_1]] \tag{120}$$

$$H_{\rm DK5} = H_{\rm DK4} + \frac{1}{24}[W_1, [W_1, [W_1, [W_1, E_1]]]] - \frac{1}{3}[W_2, [W_1, [W_1, [W_1, \beta E_p]]]] \tag{121}$$

where

$$W_1(p, p') = \beta \frac{O_1(p, p')}{E_{p'} + E_p} \tag{122}$$

$$W_2(p, p') = \beta \frac{[W_1, E_1]}{E_{p'} + E_p}\,. \tag{123}$$

Note that W_2 is not included in the expression of the DK3 Hamiltonian as well as the DK2 Hamiltonian. This can simplify the practical calculation since the evaluation of the terms including the higher order W_n becomes complicated. The third-order DK term in Eq. (119) is the correction to $V_{\rm eff}(i)$, which includes the operator, $\mathbf{p} \cdot V_{\rm ext}\mathbf{p}$. The $\mathbf{p} \cdot V_{\rm ext}\mathbf{p}$ operator may be reduced to the operator including the delta function when $V_{\rm ext}$ is a Coulomb potential. Thus, the third-order DK term affects the s orbitals, since the s orbitals have no node at the nucleus.[116]

The DK transformation correct to second order in the external potential (DK2) has been extensively studied by Hess and co-workers,[105] and has become one of the most familiar quasi-relativistic approaches. A numerical analysis by Molzberger and Schwarz[117] shows that the DK2 method recovers energy up to the order of $Z^6\alpha^4$ to a large extent and includes also a significant part of the higher-order terms. However, the DK2 approach does not completely recover the stabilizing higher-order energy contributions, as shown previously.[103] The DK3 approach improves this deficiency to a large extent.

While the DK formulas for the one-electron system are represented so far, the resulting formulas can be easily extended to the many-electron systems with the no-pair theory.[118] The explicit expression for the DK3 Hamiltonian is given in Ref. 116. The DK approach has several advantages. It is variationally stable and can avoid the Coulomb singularity. The DK method can be easily incorporated into any kind of *ab initio* and DFT theory, as well as the RESC method. Thus, one can handle the relativistic effect on the same footing with the electron correlation effect. We stress that modification of the one-electron integrals for the third-order relativistic correction with the DK3 Hamiltonian is not expensive in comparison with the DK2 Hamiltonian.

We have applied the DK3 approach to several atomic and molecular systems and confirm that the DK3 method gives excellent results.[103,116,119–124] The DK and RESC methods are currently implemented in several *ab initio* MO programs. The second-order DK (DK2) method can be used in the MOLCAS and Dalton programs. The NWChem and GAMESS programs will be able to treat the DK3 method, as well as the DK2 and RESC methods, in their forthcoming versions. The relativistic basis sets for the DK3 method[121,122] and the model potentials with the DK3 method[123,124] are prepared. Thus, we expect that the relativistic effect becomes closer to various chemists.

3.3. *Benchmark calculation*

The benchmark calculations of the spectroscopic values of Au_2 molecule in the ground state[84] were performed to demonstrate the performance of the DK3 relativistic correction in comparison with the four-component DHF and DKS calculations of REL4D. The same quality of basis sets [29s25p15d11f]/(11s8p5d3f) was used for the direct comparisons between DK3 and four-component calculations. The DFT calculations employed the BLYP exchange-correlation functional. The spin-free part of the DK3 Hamiltonian was used, and the spin-dependent term was not considered. Table 4 shows the bond lengths,

Table 4. Equilibrium internuclear distances, harmonic vibrational frequencies, and dissociation energies of Au_2 in its ground state.

	r_e (Å)	ω_e (cm^{-1})	D_e (eV)
DK3-HF	2.603	164	0.850
4-component DHF	2.594	164	0.890
DK3-KS (BLYP)	2.552	173	2.051
4-component DKS (BLYP)	2.549	173	2.230
Exptl.[a]	2.472	191	2.36

[a]Refs. 125 and 126.

vibrational frequencies, and dissociation energies of Au_2. The DK3 calculations give good performances in comparison with the corresponding four-component calculations. The bonds are stretched by about 0.009 Å (HF) and 0.003 Å (DFT). The harmonics vibrational frequencies are exactly similar. The dissociation energies are decreased by about 0.04 eV (HF) and 0.18 eV (DFT). The discrepancies between spin-free DK3 and the four-component calculations values seemed to be caused mainly from the treatment of the spin-orbit coupling. The discrepancies between the relativistic DFT calculations and experimental values seem to be affected by the problem of the exchange-correlation functional obtained in the non-relativistic formalism. Thus, we may have to develop the relativistic exchange-correlation functional for an accurate description of the heavy-element systems.

Theory and algorithms discussed in this review have been incorporated into "*UTChem*". *UTChem* is a program package for molecular simulations and dynamics developed in our group at the University of Tokyo. It is based on the very efficient integral package "Spherica"[97] and composed of various programs of *ab initio* MO methods, DFT, relativistic molecular theory, *ab initio* dynamics, hybrid QM/MM, etc. The program will be released in the near future.

Acknowledgments

This research was supported in part by a grant-in-aid for Scientific Research in Priority Areas "Molecular Physical Chemistry" from the Ministry of Education, Science, Culture, and Sports of Japan, and by a grant from the Genesis Research Institute.

References

1. K. Hirao, *Chem. Phys. Lett.* **190**, 374 (1992).
2. K. Hirao, *Chem. Phys. Lett.* **196**, 397 (1992).
3. K. Hirao, *Int. J. Quant. Chem.* **S26**, 517 (1992).
4. K. Hirao, *Chem. Phys. Lett.* **201**, 59 (1993).
5. H. Nakano, *J. Chem. Phys.* **99**, 7983 (1993).
6. H. Nakano, *Chem. Phys. Lett.* **207**, 372 (1993).
7. P.E. Siegbahn, A. Heiberg, B.O. Roos and B. Levy, *Physica Scripta* **21**, 323 (1980).
8. B.O. Roos, P.R. Taylor and P.E. Siegbahn, *Chem. Phys.* **48**, 157 (1980).
9. B.O. Roos, *Int. J. Quant. Chem.* **S14**, 175 (1980).
10. H. Nakano and K. Hirao, *Chem. Phys. Lett.* **317**, 90 (2000).
11. H. Nakano, J. Nakatani and K. Hirao, *J. Chem. Phys.* **114**, 1133 (2001).
12. H. Nakano, R. Uchiyama and K. Hirao, *J. Comput. Chem.*, in press.
13. Y.-K. Choe, Y. Nakao and K. Hirao, *J. Chem. Phys.* **115**, 621 (2001).
14. P. Celani and H.-J. Werner, *J. Chem. Phys.* **112**, 5546 (2000).
15. B. Huron, J.-P. Malrieu and P. Rancurel, *J. Chem. Phys.* **58**, 5745 (1973).
16. V.N. Staroverov and E.R. Davidson, *Chem. Phys. Lett.* **296**, 435 (1998).
17. P. Celani and H.-J. Werner, *J. Chem. Phys.* **112**, 5546 (2000).
18. R.B. Murphy and R.P. Messmer, *Chem. Phys. Lett.* **183**, 443 (1991).
19. S. Grimme and M. Waletzke, *Phys. Chem. Chem. Phys.* **2**, 2075 (2000).
20. R. Cimiraglia, *J. Chem. Phys.* **83**, 1746 (1985).
21. R. Krishnan, J.S. Binkley, R. Seeger and J.A. Pople, *J. Chem. Phys.* **72**, 650 (1980).
22. K. Yamada, T. Nakagawa and Y. Morino, *J. Mol. Spectrosc* **38**, 70 (1971).
23. T.H. Dunning, Jr., *J. Chem. Phys.* **90**, 1007 (1989).
24. M.R.J. Hachey, P.J. Bruna and F.J. Grein, *J. Phys. Chem.* **99**, 8050 (1995).
25. M. Merchán and B.O. Roos, *Theor. Chim. Acta.* **92**, 227 (1995).
26. S.R. Gwaltney and R.J. Bartlett, *Chem. Phys. Lett.* **241**, 26 (1995).
27. Y. Nakao, Y.K. Choe and K.Hirao, *Mol. Phys.* **100**, 729 (2002).
28. H. Larsen, J. Olsen, P. Jørgensen and O. Christiansen, *J. Chem. Phys.* **113**, 6677 (2000).
29. T.H. Dunning, Jr. and R.J. Harrison, *J. Chem. Phys.* **96**, 6796 (1992).
30. T. Hashimoto, H. Nakano and K. Hirao, *J. Mol. Struct.* (*Theochem*), **451**, 25 (1998).
31. A. Hiraya and K. Shobatake, *J. Chem. Phys.* **94**, 7700 (1991)
32. N. Nakashima, H. Inoue, M. Sumitani and K. Yoshihara, *J. Chem. Phys.* **73**, 5976 (1980).

33. J.P. Doering, *J. Chem. Phys.* **51**, 2866 (1969).
34. R. Astier and Y.H. Meyer, *Chem. Phys. Lett.* **3**, 399 (1969).
35. W. Kohn and L.J. Sham, *Phys. Rev.* **A140**, 1133 (1965).
36. R.G. Parr and W. Yang, *Density-Functional Theory of Atoms and Molecules* (Oxford University Press, New York, 1989).
37. R.M. Dreizler and E.K.U. Gross, *Density-Functional Theory: An Approach to the Quantum Many-Body Problem* (Springer-Verlag, Berlin, Heidelberg, 1990).
38. Q.S. Zhao, R.C. Morrison and R.G. Parr, *Phys. Rev.* **A50**, 2138 (1994).
39. P.R.T. Schipper, O.V. Gritsenko and E.J. Baerends, *Phys. Rev.* **A57**, 1729 (1998).
40. J.P. Perdew and Y. Wang, *Electronic Strucure of Solids '91*, eds. P. Ziesche and H. Eschrig (Akademie Verlag, Berlin, 1991).
41. J.P. Perdew, K. Burke and M. Ernzerhof, *Phy. Rev. Lett.* **77**, 3865 (1996).
42. A.D. Becke, *Phys. Rev.* **A38**, 3098 (1988).
43. C. Lee, W. Yang and R.G. Parr, *Phys. Rev.* **B37**, 785 (1988).
44. T. Tsuneda and K. Hirao, *Phys. Rev.* **B62**, 15527 (2000).
45. T. Tsuneda, T. Suzumura and K. Hirao, *J. Chem. Phys.* **110**, 10664 (1999).
46. T. Tsuneda and K. Hirao, *Chem. Phys. Lett.* **268**, 510 (1997).
47. T. Tsuneda, M. Kamiya, N. Morinaga and K. Hirao, *J. Chem. Phys.* **114**, 6505 (2001).
48. J.P. Perdew and A. Zunger, *Phys. Rev.* **B23**, 5048 (1981).
49. B.G. Johnson, C.A. Gonzales, P.M.W. Gill and J.A. Pople, *Chem. Phys. Lett.* **221**, 100 (1994).
50. X. Tong and S. Chu, *Phys. Rev.* **A55**, 3406 (1997).
51. T. Tsuneda, M. Kamiya and K. Hirao, submitted.
52. M. Kamiya, T. Tsuneda and K. Hirao, submitted.
53. H. Iikura, T. Tsuneda, T. Yanai and K. Hirao, *J. Chem. Phys.* **115**, 3540 (2001).
54. J.P. Perdew and Y. Wang, *Phys. Rev.* **B45**, 13244 (1992).
55. S.H. Vosko, L. Wilk and M. Nusair, *Can. J. Phys.* **58**, 1200 (1980).
56. J.W. Negele and D. Vautherin, *Phys. Rev.* **C5**, 1472 (1972).
57. R.M. Koehl, G.K. Odom and G.E. Scuseria, *Mol. Phys.* **87**, 835 (1996).
58. T.V. Voorhis and G.E. Scuseria, *Mol. Phys.* **92**, 601 (1997).
59. R. van Leeuwen and E.J. Baerends, *Phys. Rev.* **A49**, 2421 (1994).
60. M. Levy, J.P. Perdew and V. Sahni, *Phys. Rev.* **A30**, 2745 (1984).
61. T. Tsuneda and K. Hirao, *Reviews in Modern Quantum Chemistry: A Celebration of the Contributions of R. G. Parr*, ed. K.D. Sen (World Scientific, Singapore, 2002), in press.
62. R. Colle and O. Salvetti, *Theoret. Chim. Acta* **37**, 329 (1975).
63. A.K. Rajagopal, J.C. Kimball and M. Banerjee, *Phys. Rev.* **B18**, 2339 (1978).
64. A.K. Rajagopal, *Adv. Chem. Phys.* **41**, 59 (1980).
65. A.D. Becke, *J. Chem. Phys.* **88**, 1053 (1988).
66. S. Yanagisawa, T. Tsuneda and K. Hirao, *J. Chem. Phys.* **112**, 545 (2000).
67. S. Yanagisawa, T. Tsuneda and K. Hirao, *J. Comput. Chem.* **22**, 1995 (2001).
68. http://www.accelrys.com/cerius2/dmol3.html.
69. G. te Velde, F.M. Bickelhaupt, E.J. Baerends, C.F. Guerra, S.J.A. van Gisbergen, J.G. Snijders and T. Ziegler, *J. Comp. Chem.* **22**, 931 (2001); http://www.scm.com/.
70. http://www.msg.ameslab.gov/GAMESS/-GAMESS.html.
71. N.H. March, *Phys. Rev.* **A36**, 5077 (1987).
72. J. Tao, *J. Chem. Phys.* **115**, 3519 (2001).
73. J.K. Kan and C.B. Musgrave, *J. Chem. Phys.* **115**, 11040 (2001).
74. A. Savin, *Recent Developments and Applications of Modern Density Functional Theory*, ed. J. M. Seminario (Elsevier, Amsterdam, 1996), p. 327.
75. T. Leininger, H. Stoll, H.-J. Werner and A. Savin, *Chem. Phys. Lett.* **275**, 151 (1997).
76. R.D. Adamson, J.P. Dombroski and P.M.W. Gill, *J. Comput. Chem.* **20**, 921 (1999).
77. Y. Andersson, D.C. Langreth and B.I. Lundqvist, *Phys. Rev. Lett.* **76**, 102 (1996).
78. R. Krishnan, J.S. Binkley, R. Seeger and J.A. Pople, *J. Chem. Phys.* **72**, 650 (1980).
79. A.D. McLean and G.S. Chandler, *J. Chem. Phys.* **72**, 5639 (1980).
80. M.J. Frisch, J.A. Pople and J.S. Binkley, *J. Chem. Phys.* **80**, 3265 (1984).
81. S.F. Boys and F. Bernardi, *Mol. Phys.* **19**, 553 (1970).
82. C. Adamo and V. Barone, *J. Chem. Phys.* **118**, 664 (1998).
83. Q. Wu and W. Yang, *J. Chem. Phys.* **116**, 515 (2002).
84. T. Nakajima, T. Yanai and K. Hirao, *J. Comput. Chem.* **23**, 847 (2002).
85. A.K. Rajagopal and J. Callaway, *Phys. Rev.* **B7**, 1912 (1973).
86. A.K. Rajagopal, *J. Phys.* **C11**, L943 (1978); A.K. Rajagopal, *Phys. Rev.* **A50**, 3759 (1994).
87. A.H. MacDonald and S.H. Vosko, *J. Phys.* **C12**, 2977 (1979).
88. S. Varga, E. Engel, W.-D. Sepp and B. Fricke, *Phys. Rev.* **A59**, 4288 (1999).
89. W. Liu, G. Hong, D. Dai, L. Li and M. Dolg, *Theor. Chiem. Acc.* **96**, 75 (1997).

90. L. Visscher, O. Visser, H. Aerts, H. Merenga and W.C. Nieuwpoort, *Comput. Phys. Commun.* **81**, 120 (1994).
91. T. Saue, K. Fægrei, T. Helgaker and O. Gropen, *Mol. Phys.* **91**, 937 (1997).
92. H.M. Quiney, H. Skaane and I.P. Grant, *Adv. Quant. Chem.* **32**, 1 (1999); I.P. Grant and H.M. Quiney, *Int. J. Quant. Chem.* **80**, 283 (2000).
93. T. Yanai, T. Nakajima, Y. Ishikawa and K. Hirao, *J. Chem. Phys.* **114**, 6526 (2001).
94. T. Yanai, H. Iikura, T. Nakajima, Y. Ishikawa and K. Hirao, *J. Chem. Phys.* **115**, 8267 (2001).
95. T. Yanai, T. Nakajima, Y. Ishikawa and K. Hirao, *J. Chem. Phys.* **116**, 10122 (2002).
96. Y. Ishikawa, R.C. Binning and K.M. Sando, *Chem. Phys. Lett.* **101**, 111 (1983); **105**, 189 (1984); **117**, 444 (1985); Y.S. Lee and A.D. McLean, *J. Chem. Phys.* **76**, 735 (1982); H. Aerts and W.C. Nieuwpoort, *Chem. Phys. Lett.* **113**, 165 (1985); R.E. Stanton and S. Havriliak, *J. Chem. Phys.* **81**, 1910 (1984).
97. T. Yanai, K. Ishida, H. Nakano and K. Hirao, *Int. J. Quant. Chem.* **76**, 396 (2000).
98. K. Ishida, *Int. J. Quant. Chem.* **59**, 209 (1996); K. Ishida, *J. Chem. Phys.* **109**, 881 (1998); K. Ishida, *J. Comput. Chem.* **19**, 923 (1998); K. Ishida, *J. Chem. Phys.* **111**, 4913 (1999); K. Ishida, *ibid.* **113**, 7818 (2000).
99. H.A. Bethe and E.E. Salpeter, *Quantum Mechanics of One- and Two-Electron Atoms* (Springer, Berlin, Heidelberg, New York, 1957).
100. L.L. Foldy and S.A. Wouthuysen, *Phys. Rev.* **78**, 29 (1950).
101. E. van Lenthe, E.J. Baerends and J.G. Snijders, *J. Chem. Phys.* **99**, 4597 (1993); Ch. Chang, M. Pelissier and Ph. Durand, *Phys. Scr.* **34**, 394 (1986).
102. T. Nakajima and K. Hirao, *Chem. Phys. Lett.* **302**, 383 (1999).
103. T. Nakajima and K. Hirao, *J. Chem. Phys.* **113**, 7786 (2000).
104. R.J. Buenker, P. Chandra and B.A. Hess, *Chem. Phys.* **84**, 1 (1984).
105. B.A. Hess, *Phys. Rev.* **A33**, 3742 (1986); G. Jansen and B.A. Hess, *Phys. Rev.* **A39**, 6016 (1989).
106. T. Nakajima, T. Suzumura and K. Hirao, *Chem. Phys. Lett.* **304**, 271 (1999).
107. T. Suzumura, T. Nakajima and K. Hirao, *Int. J. Quant. Chem.* **75**, 757 (1999).
108. Y.-K. Choe, T. Nakajima, K. Hirao and R. Lindh, *J. Chem. Phys.* **111**, 3837 (1999).
109. H.A. Witek, T. Nakajima and K. Hirao, *J. Chem. Phys.* **113**, 8015 (2000).
110. T. Nakajima, K. Koga and K. Hirao, *J. Chem. Phys.* **112**, 10142 (2000).
111. S. Yanagisawa, T. Nakajima, T. Tsuneda and K. Hirao, *Theochem*, **537**, 63 (2001).
112. Y. Kayaki, H. Tsukamoto, M. Kaneko, I. Shimizu, A. Yamamoto, M. Tachikawa and T. Nakajima, *J. Organometallic Chem.* **622**, 199 (2001).
113. K. Motegi, T. Nakajima, K. Hirao and L. Seijo, *J. Chem. Phys.* **114**, 6000 (2001).
114. D. Fedorov, T. Nakajima and K. Hirao, *Chem. Phys. Lett.* **335**, 183 (2001).
115. M. Douglas and N.M. Kroll, *Ann. Phys.* (New York) **82**, 89 (1974).
116. T. Nakajima and K. Hirao, *Chem. Phys. Lett.* **329**, 511 (2000).
117. K. Molzberger and W.H.E. Schwarz, *Theor. Chim. Acta* **94**, 213 (1996).
118. J. Sucher, *Phys. Rev.* **A22**, 348 (1980).
119. T. Nakajima and K. Hirao, *Chem. Lett.* **766** (2001).
120. S. Ikeda, T. Nakajima and K. Hirao, *Mol. Phys.*, in press.
121. T. Tsuchiya, M. Abe, T. Nakajima and K. Hirao, *J. Chem. Phys.*, **115**, 4463 (2001).
122. T. Nakajima and K. Hirao, *J. Chem. Phys.* **116**, 8270 (2002).
123. J. Paulovic, T. Nakajima, K. Hirao and L. Seijo, *J. Chem. Phys.*, in press.
124. T. Tsuchiya, T. Nakajima, K. Hirao and L. Seijo, *Chem. Phys. Lett.*, in press.
125. K.P. Huber and G. Herzberg, *Molecular Structure IV, Constants of Diatomic Molecules* (Van Nostrand, New York, 1979).
126. B. Simard and P.A. Hackett, *J. Mol. Spectrosc.* **412**, 310 (1990).